SOME STUDIES ON THE DYNAMIC MECHANICAL PROPERTIES OF SYNTHETIC EGG ALBUMIN AND ACETATE RAYON FIBERS

by

ALAN DAVID McINTYRE

A THESIS SUBMITTED IN PARTIAL FULFILMENT OF
THE REQUIREMENTS FOR THE DEGREE OF

MASTER OF ARTS

in the Department

of

CHEMISTRY

We accept this thesis as conforming
to the standard required from candidates
for the degree of MASTER OF ARTS.

Members of the Department of
Chemistry

THE UNIVERSITY OF BRITISH COLUMBIA

April, 1952

ABSTRACT

The dynamic mechanical properties of egg albumin and acetate rayon fibers have been discussed in terms of the theories of Tobolsky, Dunell and Andrews (18) and Kuhn, Kunzle and Preissman (17).

The dependence of these properties on relative humidity has been determined for a series of relative humidities from 27 to 82% RH. The variation of the energy loss factor, $\omega\eta(\omega)$, with relative humidity is in agreement with the present theories of dynamic properties; an increase in this factor with increased relative humidity. Less success has been attained in the correlation of the dependence of the dynamic modulus on relative humidity. It has been found that E_{dyn} of acetate is independent of relative humidity at low humidities, in agreement with the theory but is abnormally high at higher relative humidities. For the albumin fibers, it has been found that E_{dyn} decreases with increase in relative humidity. These latter effects are inexplicable in terms of the present theories.

The effects of orientation on $\omega\eta(\omega)$ of albumin fibers has been found; a decrease in the energy loss factor with increased orientation. The decrease in dynamic modulus with orientation disagrees with the result expected on the basis of the present theories of polymer systems.

ACKNOWLEDGEMENTS

The author wishes to express his appreciation and sincere thanks to Dr. B.A. Dunell for his invaluable assistance and encouragement throughout the course of this work.

The author is also grateful to the National Research Council for the gift of a Bursary and a Summer Research Grant which has made most of this work possible.

TABLE OF CONTENTS

INTRODUCTION

Although the field of high polymers is comparatively new, the technical importance of these compounds has led to a very rapid development of empirical knowledge concerning them. Since this technical importance is largely due to their unique mechanical properties, a great many investigators have been doing work in this field. Mark [1, 2] discusses qualitatively the relation of chain structure and arrangement to mechanical properties, and the application of the kinetic theory of elasticity has explained quantitatively the elastic nature of some polymers [3, 4, 5, 6, 7, 8, 9]. The object of this investigation is to study the mechanical properties (dynamic modulus, E, and dynamic viscosity, η) of synthetic fibers subjected to harmonic vibration of varying frequency. In particular, an attempt will be made to correlate these properties of egg albumin fibers with the degree of steam stretching (orientation of molecules) imparted during their manufacture and with the relative humidity and temperature under which the tests are made. It is hoped that these correlations will permit an elucidation of the relation between structure and mechanical properties of fibrous materials.

A. MECHANICAL PROPERTIES OF POLYMERS

In order to describe conveniently and predict the mechanical behaviour of systems under a variety of stress-strain conditions, the use of mechanical analogies (springs and dashpots in more or less complicated parallel and series arrays) has been widely adopted (10, 11, 12, 13). To introduce the basic concepts and necessary nomenclature a short discussion of some mechanical analogies is given below.

When a deformation has occurred, the structural units within the material have moved with respect to one another. If the substance returns to its original shape, the process is described as elastic, whereas, if permanent deformations occur, the units have moved permanently past one another and the process is described as flow.

An elastic deformation which is completely reversible is represented by a Hookean spring:

$$\frac{s}{\epsilon} = E$$

where s is the applied stress, ϵ the strain and E is Young's modulus. The variation of strain with time is illustrated in Figure 1(a) by the flow curve for an ideally elastic body and a stress-strain plot is given in Figure 1(b). An irreversible process may be represented by a dashpot containing a Newtonian fluid whose laminar flow can be described by the equation:

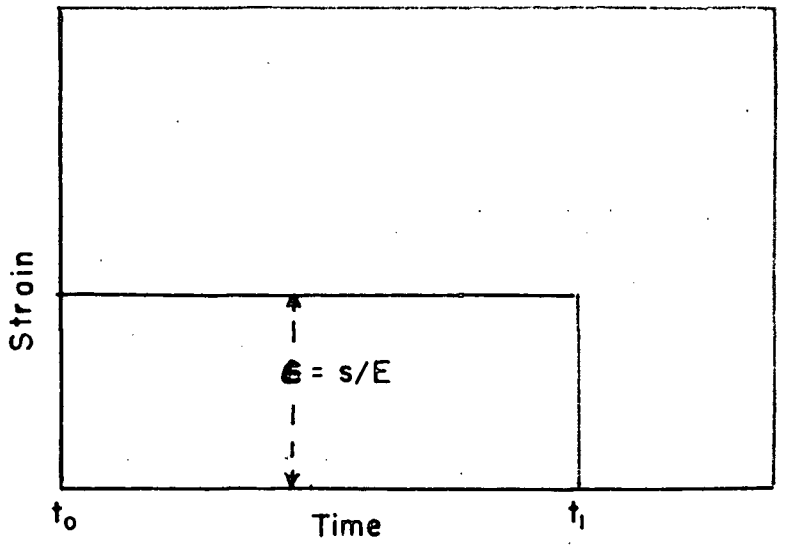

Figure Ia. A constant stress is applied at t_o and removed at t_1.

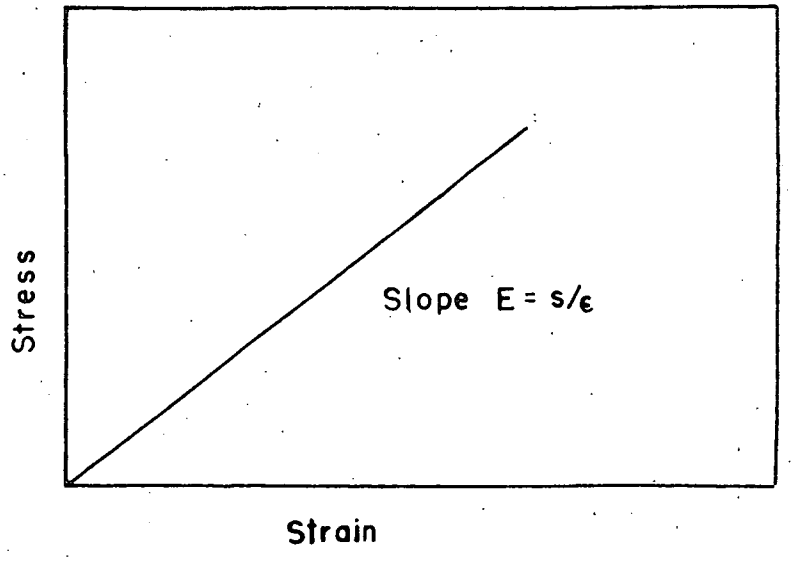

Figure Ib. Stress-Strain Diagram.

$$\frac{6}{d\xi/dt} = \eta$$

where 6 is the shear stress, $\frac{d\xi}{dt}$ the velocity gradient, and η the viscosity. Any stress acting on a dashpot produces a continually increasing strain; the strain is therefore a function of stress and time as shown in Figure 2.

It is found with most polymers that an instantaneously applied stress decays with time at constant strain, and at constant stress the strain increases with time, the former phenomenon being designated relaxation and the latter creep. The use of Voigt and Maxwell units as mechanical analogies partially describes these effects. For the Maxwell unit, shown in Figure 3(a), the rate of strain is:

$$\frac{d\epsilon}{dt} = \frac{1}{E}\frac{dS}{dt} + \frac{S}{\eta}$$

and for the Voigt unit, shown in Figure 3(b), the rate of strain is:

$$\frac{d\epsilon}{dt} = \frac{S}{\eta} - \frac{E\epsilon}{\eta}$$

At constant strain the first equation reduces to:

$$S = S_0 e^{-\frac{E}{\eta}t} = S_0 e^{-\frac{t}{\tau}}$$

where S_0 is the initial stress and τ is the relaxation time,

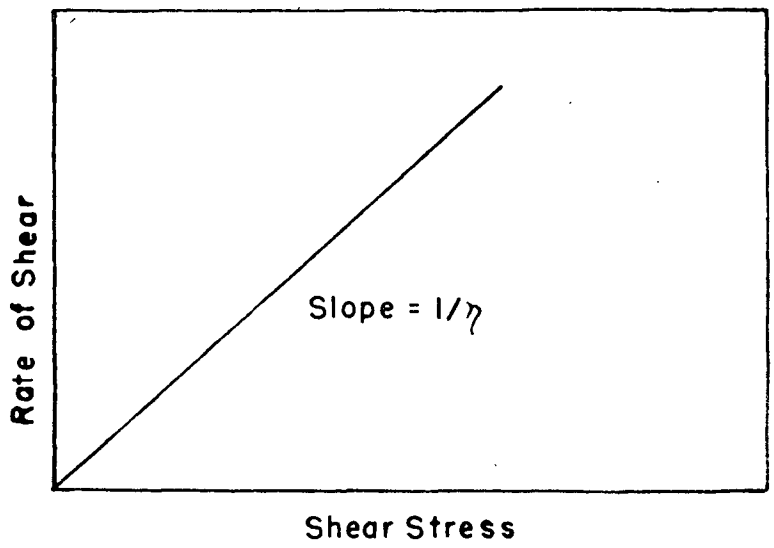

Figure 2a. Modified Stress-Strain diagram for Shear.

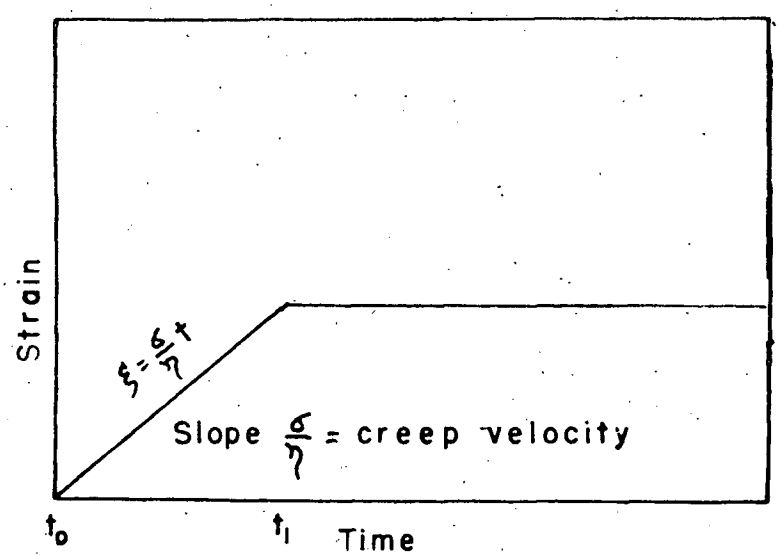

Figure 2b. A constant Shear Stress is applied at t_0 and removed at t_1. Permanent deformation.

the time required for the stress to decay to 1/e of its initial value. The parallel unit (b) will not exhibit such relaxation effects because the stress applied to attain a desired strain will depend on the rate of deformation and, once this strain is achieved, the stress remains constant at the value S. For the parallel unit the piston begins to move at a rate $\frac{S}{\eta}$ which decreases asymptotically as the stress is gradually transferred to the spring. Thus a reinforcement occurs during flow. When the initially applied stress is suddenly removed, the rate of change of strain is given by:

$$\frac{d\epsilon}{dt} = -\frac{\eta}{E}\epsilon$$

which on integration gives:

$$\epsilon = \epsilon_0 e^{-\frac{\eta}{E}t} = \epsilon_0 e^{-\frac{t}{\tau}}$$

In practice, to describe creep and relaxation phenomena, it is necessary to assume a distribution of relaxation times (14, 15). The simple expression:

$$\frac{S}{\epsilon} = E e^{-\frac{t}{\tau}}$$

is replaced by:

$$\frac{S}{\epsilon} = \sum E_i e^{-\frac{t}{\tau}}$$

Tobolsky and Eyring [16] have suggested that the behaviour of amorphous material under forced vibrations could be represented by an infinite array of Maxwell or Voigt units with dynamic parameters which are frequency dependent. Kuhn, Kunzle and Preissman [17] have shown how the dynamic parameters can be predicted from creep experiments using a logarithmic distribution of relaxation times. The mathematical analysis leading to their conclusions is presented in the Appendix. Tobolsky, Dunell and Andrews [18] have described a method of predicting the dynamic parameters from stress relaxation curves based on an extended Maxwellian relaxation theory. The relations derived for the dynamic modulus and dynamic viscosity are:

$$E_{dyn}(\omega) = \int \frac{\omega^2 \tau^2 E(\tau)}{1 + \omega^2 \tau^2} \, d\tau$$

$$\omega \eta(\omega) = \int \frac{\omega \tau E(\tau)}{1 + \omega^2 \tau^2} \, d\tau$$

$E(\tau)$ is a distribution function describing the spectrum of relaxation times. $E(\tau)d\tau$ specifies the contribution to the total instantaneous tensile modulus, E, of the system from Maxwell units having relaxation times between τ and $\tau + d\tau$ Using a distribution function of the form:

$$E(\tau) = \frac{E_0}{\tau} \qquad (\tau_l < \tau < \tau_m)$$

$$E(\tau) = 0 \qquad (\tau < \tau_l, \ \tau > \tau_m)$$

Figure 3a. Maxwell Unit.

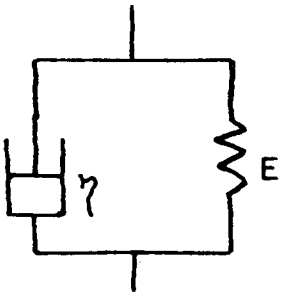

Figure 3b. Voigt Unit.

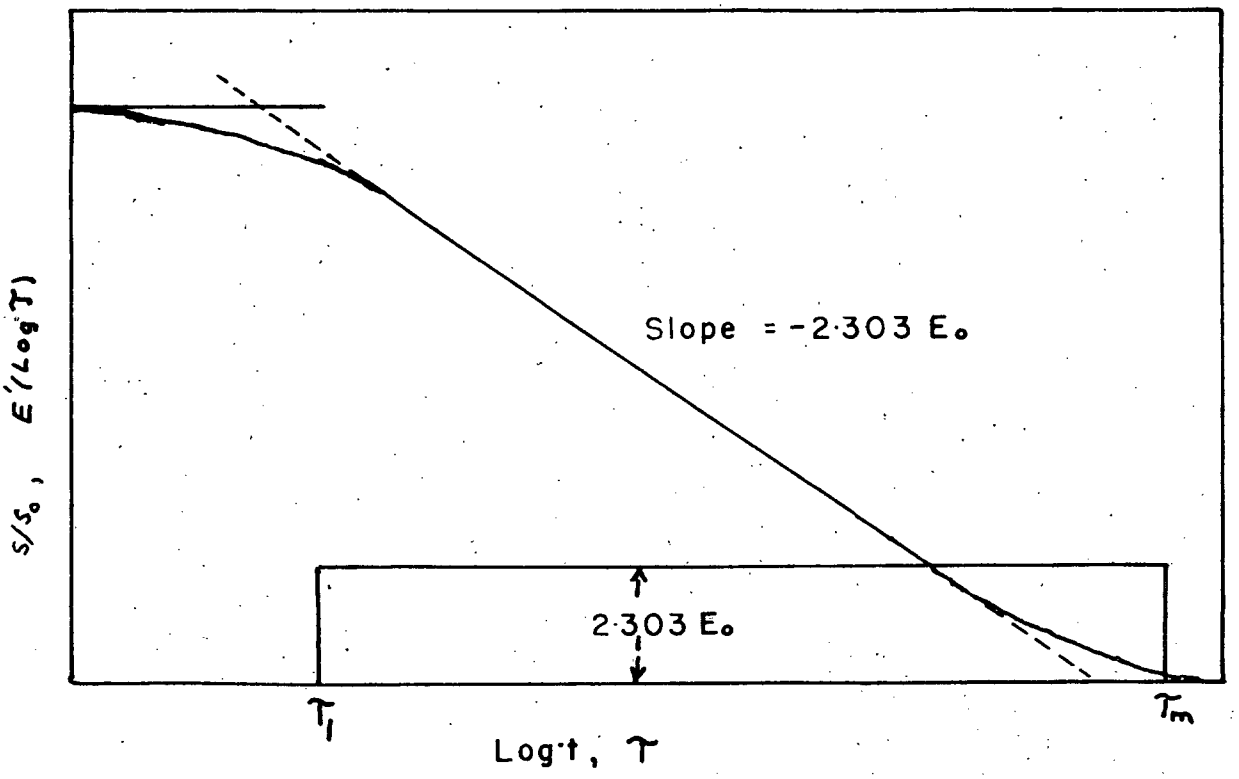

Figure 4. Stress relaxation and distribution function for a polymer.

these workers have found a good correlation between predicted and observed values of the dynamic parameters. E_o is related to the straight line portion of a logarithmic stress-relaxation curve (Figure 4) and τ_m and τ_l denote the maximum and minimum relaxation times found by extrapolation of this straight line portion.

B. SYNTHETIC PROTEIN FIBERS

The reasons that synthetic protein fibers are commercially useful are twofold: the fact that the common natural protein fibers have desirable characteristics, warmth, durability and resilience and an affinity for dyes; and the fact that the raw materials are abundant.

Proteins, being chain molecules, are structurally suitable for the formation of fibers (Figure 5). The diversity of residues and arrangement of polar side groups give rise to a great many different protein materials. Proteins are not only chains like other high polymer systems (Figure 6) but, because of the many and varied crosslinking mechanisms, exhibit high mechanical strength. The analysis for polar groups of egg albumin is given in Table I, while some structural properties are listed in Table II [19, 20, 21, 22].

Ultracentrifugal sedimentation, diffusion and viscosity studies indicate that the axial ratio of native egg albumin is about 4 to 1 (Table II) and leads one to assume that albumin in its natural state is coiled into a folded corpuscular structure which is unsuited for fiber formation.

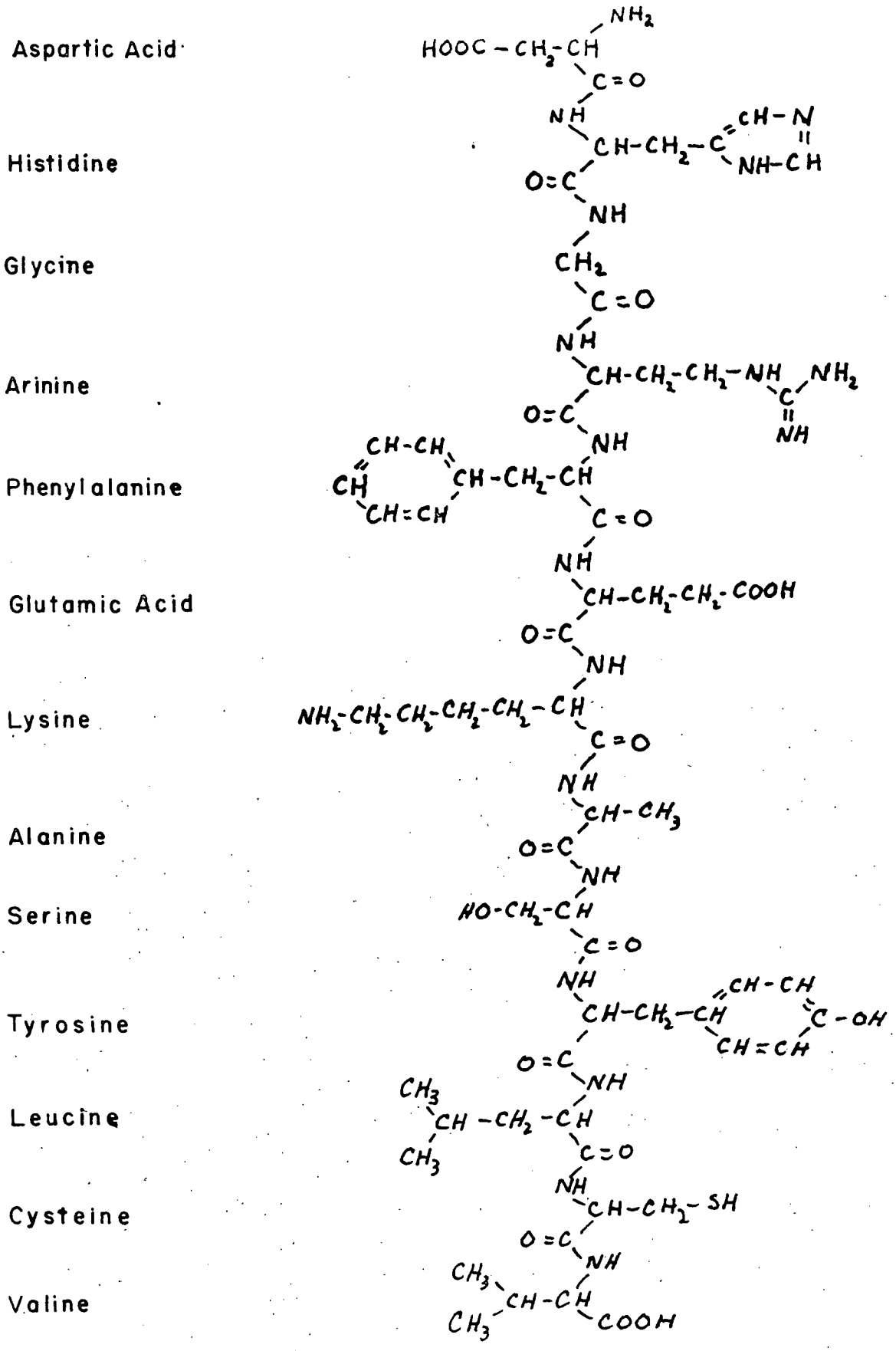

Figure 5. Chain structure of a protein.

Rubber chain

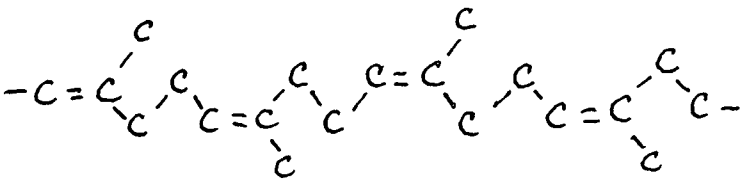

Nylon chain

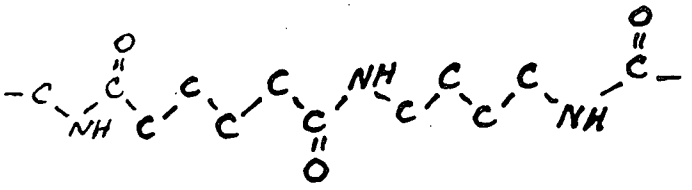

Protein chain

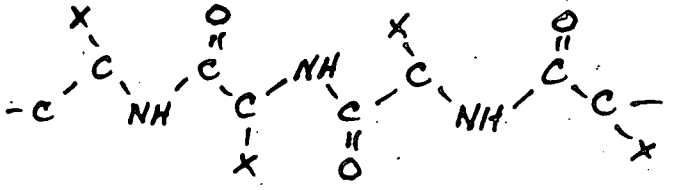

X= side chain with polar groups.

Protein

Cross-linkages

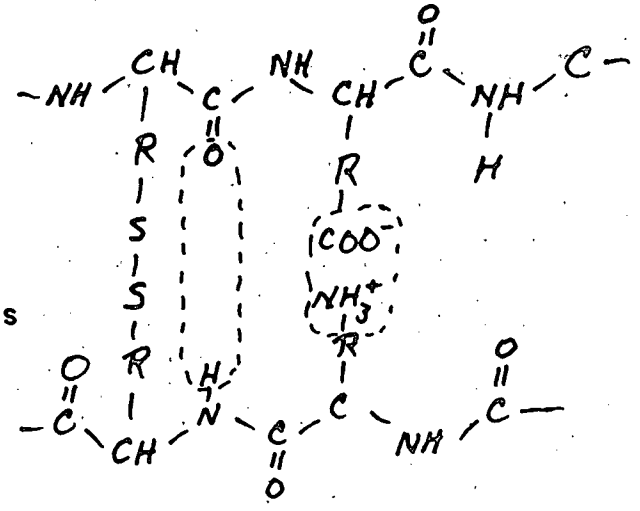

Figure 6. Comparison of a Protein skeleton with those of Rubber and Nylon, showing some possible cross-linkages.

All truly corpuscular proteins undergo denaturation very readily, the process being accompanied by unfolding of the molecules (23). Such unfolding may occur merely by letting a concentrated, electrolyte-free solution of the protein stand for a period of time. It would appear that electrostatic forces between adjacent molecules are sufficient to uncurl the corpuscles and hold them extended because, on dilution, the sedimentation rate indicates a return to a folded structure. It is obvious, therefore, that the problem of producing protein fibers reduces to the process of uncoiling the molecules and fixation in that state until suitable cross linkages have been set up (Figure 7).

When an anionic detergent, such as a long chain sulfonate, is added to a protein solution on the acid side of the isoelectric point, precipitation of the protein may occur directly. When the detergent is added on the basic side of the isoelectric point, precipitation of the protein does not occur but solutions exhibiting high viscosities result. These protein-detergent mixtures yield on precipitation by salt coagulating baths fibers which can be oriented under proper conditions. This behaviour is characteristic of both anionic and cationic detergents but not of non-ionic detergents. The fact that the lower molecular weight sulfonates do not exhibit this characteristic indicates, however, that electrostatic forces are not alone sufficient to produce a complex between proteins and detergents which can be drawn into fibers. The character of the precipitate varies with the proportion of protein to

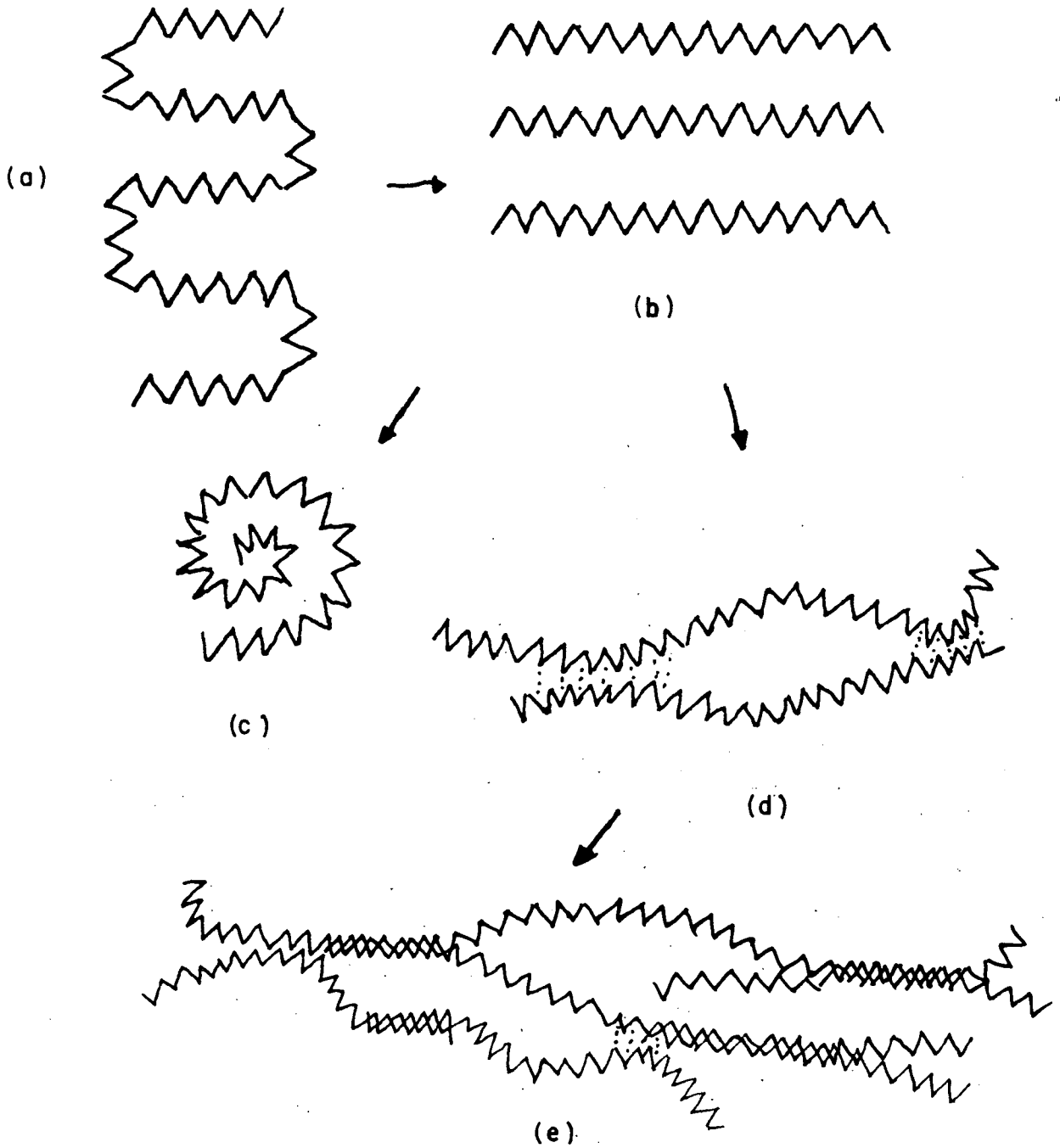

Figure 7..

(a) Corpuscular (Native) Protein.

(b) Unfolded chains.

(c) Denatured Protein (randomly folded).

(d) Orientation and cross-linking.

(e) Fiber showing amorphous and crystaline regions.

TABLE I. POLAR GROUPS OF EGG ALBUMIN

Group		Number per Molecule of 45,000 M.W.
Basic		
Imidazole	=NH	4
-amino	$-NH_2$	24
Guanidine	$-N-C(=NH)-NH_2$	15
Acidic		
Free carboxylic acid	-COOH	51
Phosphoric acid	$-O-P(=O)(OH)-OH$	1
Phenolic	- OH	9
Sulfhydryl	- SH	6
Disulfide	- S - S -	3
Amide	$-C(=O)-NH_2$	36

TABLE II. SPECIAL PROPERTIES OF EGG ALBUMIN

Molecular weight		45,000
Average amino acid residue weight		111.4
Number of residues (DP)	$\frac{45,000}{111.4}$ =	404
Total length, calculated as one chain		1,414 Å
calculated as four chains		354 Å
Cross section of single chain (X-ray)		9.5 Å

detergent, ranging from highly floculent with high protein composition to slimy residues with high detergent composition. When dried, the unoriented fibers become brittle, indicating that water is essential for flow.

Electrophoretic studies of these mixtures reveal that a complex is formed between protein and detergent. The amount of detergent that can be bound to the protein is found to be considerably in excess of that corresponding to a stoichiometric combination of the long chain salts with the basic groups of the protein molecule. With a ratio of 90 parts protein to 10 parts detergent, one finds no free detergent boundary and an analysis of the relative heights of the protein and detergent peaks indicates that the composition of the complex is approximately three parts protein to one detergent. On an ionic basis, this proportion corresponds to a ratio of one detergent ion to each basic group of the protein, indicating a stoichiometric electrostatic combination. For mixtures with about a 50-50 ratio of protein to detergent no free protein or detergent boundaries are found. In this case the stoichiometric proportions are exceeded. With a ratio of 10-90 protein-detergent one finds complex and free detergent peaks, the analysis of which shows a ratio of three parts detergent to one of protein in the complex, representing the maximum combining power of protein for detergent. For this case the combination is of the order of nine detergent ions for each basic protein group. These results are summarized in Figure 8.

Variation in concentration of solids in the three-to-

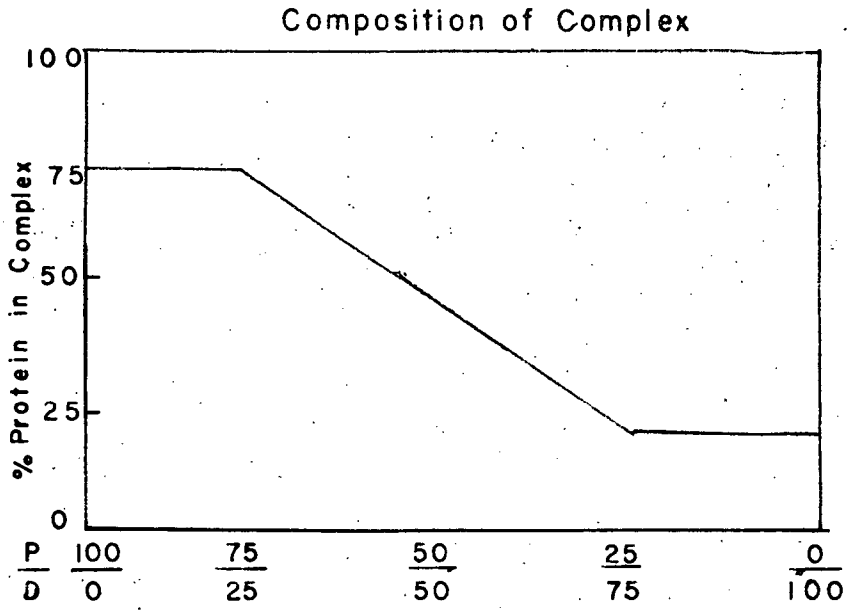

Figure 8. Variation of protein in complex with proportion by weight of albumin and nacconol used in mixtures. The region of constant proportion (3:1 by weight) at upper left corresponds to a ratio of one detergent ion for each basic group of the albumin. The region of constant composition at lower right (1:3) corresponds to about nine detergent ions for each basic group. In between (at 1:1) the complexes have flow properties desirable for making fibers.

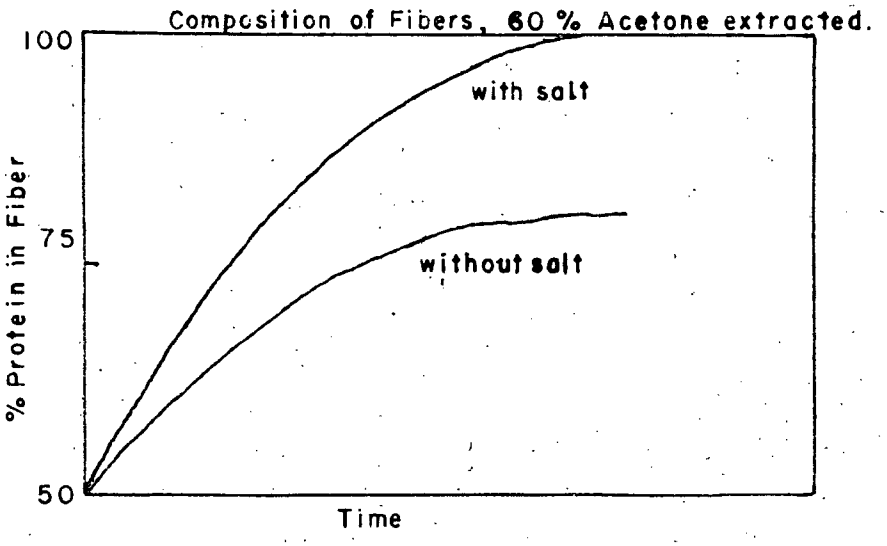

Figure 9. Recovery of detergent from 50:50 albumin:detergent complex. Using washed fibers and 60% acetone, all detergent except the 3:1 portion is removed. With electrolyte present, all detergent is extracted by the acetone.

one combining ratio has no effect on the electrophoresis data except to increase the height of the complex peak. This indicates a strong association complex is formed. The fact that non-ionic detergents will not form complexes indicates that the complexing is electrostatic in nature. This is further borne out by acetone extractions. Aqueous acetone (60-70%) will remove only the excess detergent indicating weak, non-polar binding for this portion; while extraction with 60-70% acetone containing electrolyte will remove all the bound detergent, indicating polar binding for this portion somewhat weaker than that of the salt coagulating bath. Since the detergent is not removed during the precipitation but only after 24 hours extraction in acetone, the reactions involved must be of an equilibrium nature (Figure 9). The structure of the complex proposed by Lundgren [19] is shown in Figure 10. It is easily seen from Figure 11 that water is essential for the flow properties of the albumin-detergent complex.

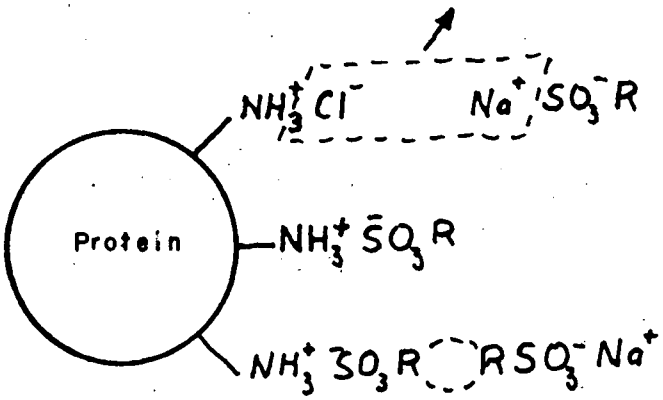

Figure 10. Diagramatic representation of albumin-detergent complex formation.

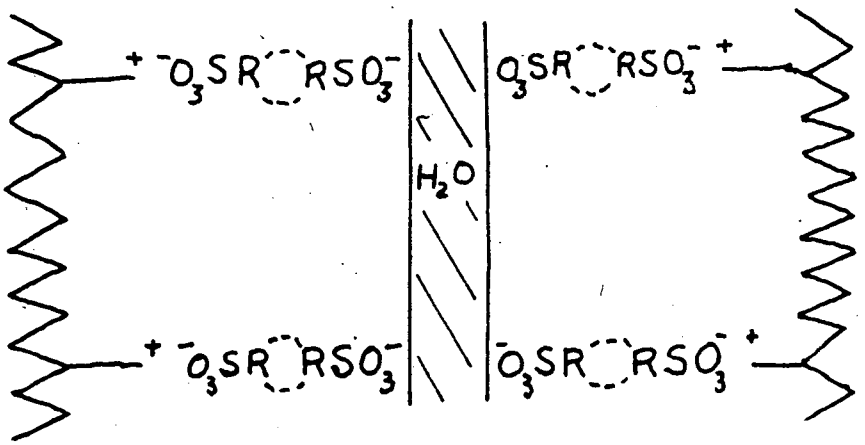

Figure 11. Proposed structure of complex (Lundgren).

The extra bound detergent gives rise to a distribution of similarly charged groups along the protein chain which favors flow.

EXPERIMENTAL METHODS AND RESULTS

A. PREPARATION OF FIBERS

The technique and equipment for the production of the egg albumin fibers are very simple. Solutions of dried albumin and purified nacconol containing 25% by weight of solids are made up in 0.1% mercaptoethanol (to prevent gelation). These solutions are mixed with rapid stirring and the resultant viscous mixture is aged overnight in a vacuum dessicator (to deareate it). The coagulating bath used is a saturated magnesium sulfate solution acidified to pH 2 with formic acid.

The spinning "dope" is extruded by means of a brass hypodermic syringe, its needle being thrust through a rubber stopper at the bottom of a glass tube containing the coagulating solution. After about five minutes the fiber is removed from the salt solution, rinsed superficially in water and then dried with infrared lamps until it no longer stretches under its own weight. A small weight is attached to the end of the fiber and the fiber is then lowered into 70% aqueous acetone saturated with coagulating salt.

After extraction with acetone for 24 hours the fibers are dried under tension and then elongated in steam. It is during this step that the desired degrees of molecular orientation is attained since, according to Lundgren [31], flow without orientation occurs when detergent is present. The fiber is then

dried under tension and is ready for testing.

It has been found that a No. 20 hypodermic needle gives a precipitated fiber of a size most readily managed with the equipment used. Precipitation of less than five minutes yields a fiber which is too slimy to handle in that it tends to elongate and break during the drying procedure, while more than ten minutes appears to reduce the tendency to flow almost to zero even in the acetone bath. Fibers precipitated for about five minutes elongate only slightly during drying (10-20%) and appear to have the most suitable characteristics for the subsequent steps. One must be careful to have the steam well distributed in the tower or else opaque unoriented patches will be obtained. These patches become extremely brittle on drying and, of course, make the whole fiber quite useless. Variations in cross sectional area along the length of the fibers are remarkably slight, the average diameter being about 0.10 mm.

B. MECHANICAL PROPERTIES

1. Vibrator

The apparatus used in this investigation is very similar to that used by Lyons and Prettyman [24] and by Dunell and Dillon [25]. It is a forced vibrator for oscillating single high polymer filaments longitudinally. A detailed plan of the oscillator is given in Figure 12, accompanied by photographs of the finished apparatus. The driving mechanism consists of a solenoid of fine Formex magnet wire wound on a paper core which is cemented to a disk and spindle machined from a piece of magnesium.

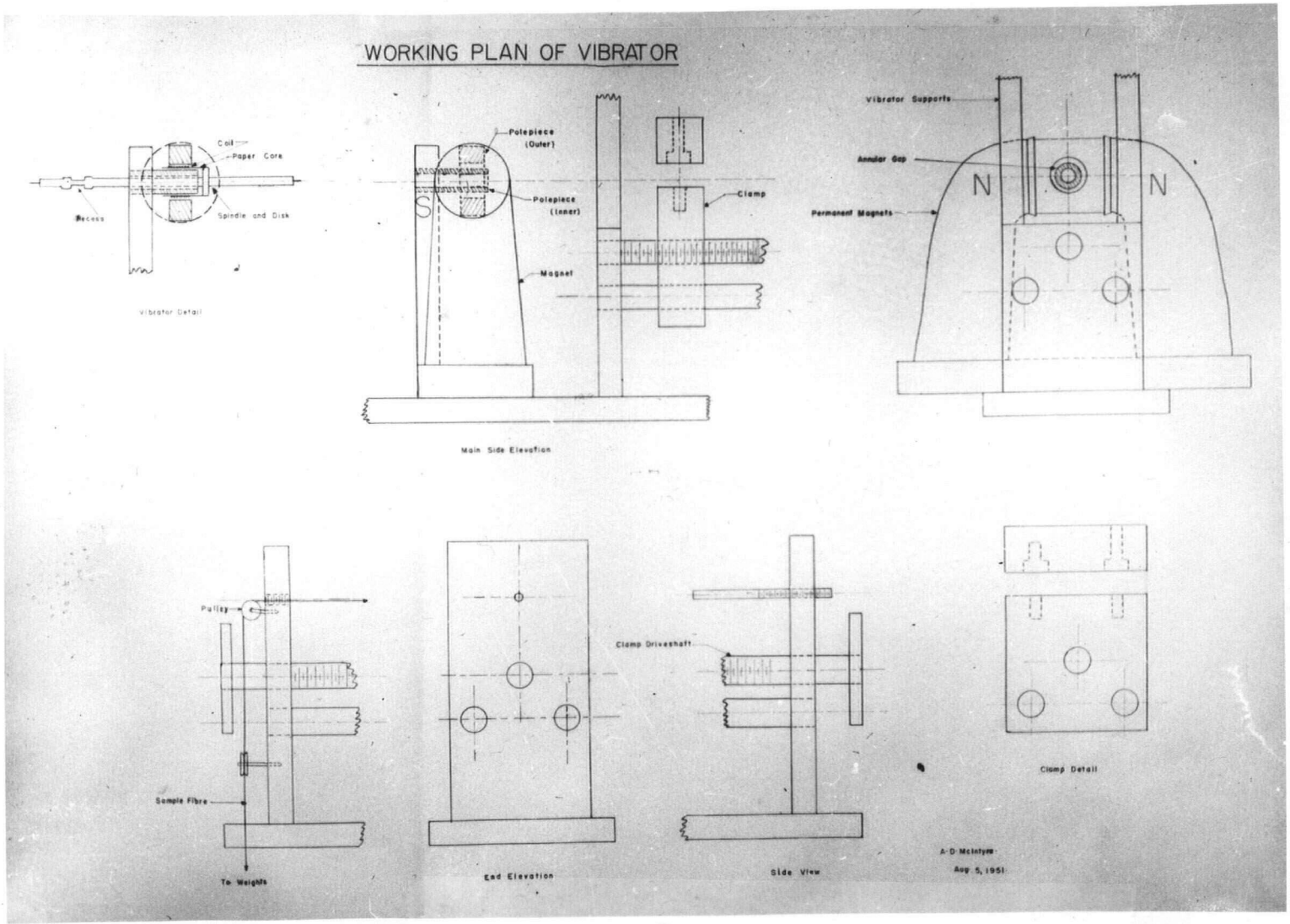
WORKING PLAN OF VIBRATOR
Coil
Paper Core
Recess
Spindle and Disk
Vibrator Detail
Polepiece (Outer)
Polepiece (Inner)
Clamp
Magnet
S
Main Side Elevation
Vibrator Supports
Annular Gap
Permanent Magnets
N
N
Pulley
Sample Fibre
To Weights
End Elevation
Clamp Driveshaft
Side View
Clamp Detail
A. D. McIntyre
Aug. 5, 1951

Figure 12.

Figure 12.

(a) Magnet and vibrator.

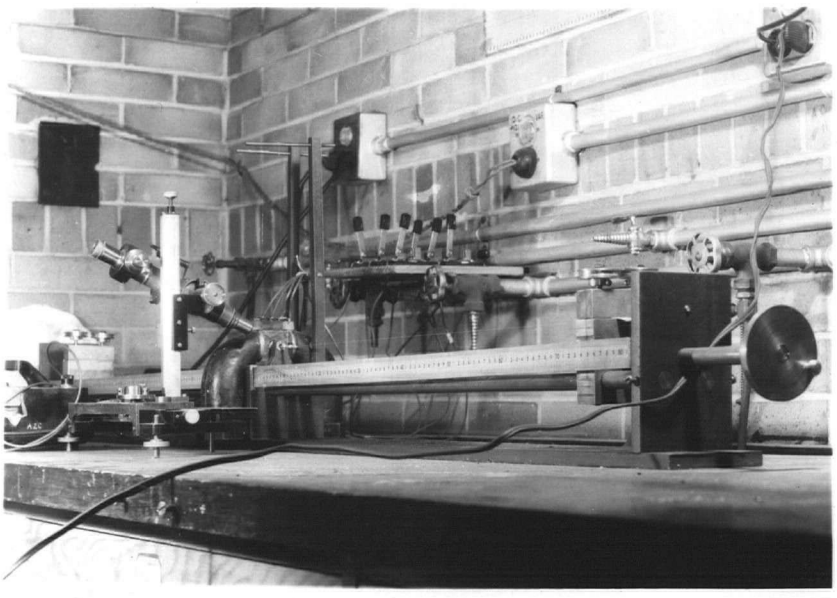

(b) Complete Apparatus.

The solenoid lies in a radial magnetic field, the spindle being supported at each end by fine nylon filaments which can be adjusted so as to center the unit in the field and ensure that there is no contact between the coil and the sides of the annular gap in which it is located. The whole vibrator unit weighs about 2.5 grams and is coated with a thin layer of polystyrene "Q Dope" to reduce the oxidation of the magnesium spindle. The coil is supplied with an alternating current from a variable frequency Hewlett-Packard oscillator through leads of the same wire that forms the winding, coiled into small helical springs to allow free motion of the vibrator unit. The magnetic field is maintained by two powerful permanent magnets, two similar poles, N, facing one another on the outer circumference of the radial gap and the steel cylinder forming the inner circumference. The filaments which are to be tested are cemented to the ends of the spindle. The other end of the right-hand filament is fastened to a movable rod and the other end of the left filament passes over the pullies and supports the tensioning weight. The filaments may be clamped at any point along their length by means of the movable clamps.

The amplitude of vibration is determined by means of a cathetometer which reads to within 0.0002 cm. the apparent increase in length during vibration of the length of the recessed portion of the spindle. The current supplied to the solenoid is recorded by a Weston Thermomiliammeter.

Two coils were made during the construction of the apparatus. The coil of the first had effectively three windings

with about 250, 15 and 2 turns per winding. Actually the winding is a single coil with two extra taps to it, so that there are only four leads in all to the coil. Since the amplitudes obtainable with this coil were too small, a second was made with 600, 50 and 5 turns per winding.

Since the vibrator unit of this oscillator is very light, the machine can be used for very fine single filaments up to fairly high resonant frequencies.

The apparatus is covered with a cabinet having a double thickness of glass separated by a 1/8 inch dead air space to permit temperature control. Holes in each end of the cabinet permit the clamp drive-shaft to be turned to allow the clamps to be adjusted from the outside. Pulleys are fixed to the bolts of the clamps (See photograph) over which strong cords are looped and passed out through other holes in the cabinet ends to enable one to loosen and tighten the clamps from the outside also. Thus, one is able to change the length of fiber being tested without disturbing the humidity conditions inside the cabinet.

The humidifying apparatus is shown in the accompanying figure. It consists of a drying tower containing silica gel. From this tower, the dry air is split into two streams, one going to a packed tower submerged in a thermostatically controlled bath where the air is saturated with water vapor and thence to a mixing chamber to which the other stream goes directly. By means of flowmeters the ratio of dry to saturated air is controlled to give the desired humidity to the air leaving the mixing chamber. From there the air is taken to the cabinet where

Figure 13. Humidification Apparatus.

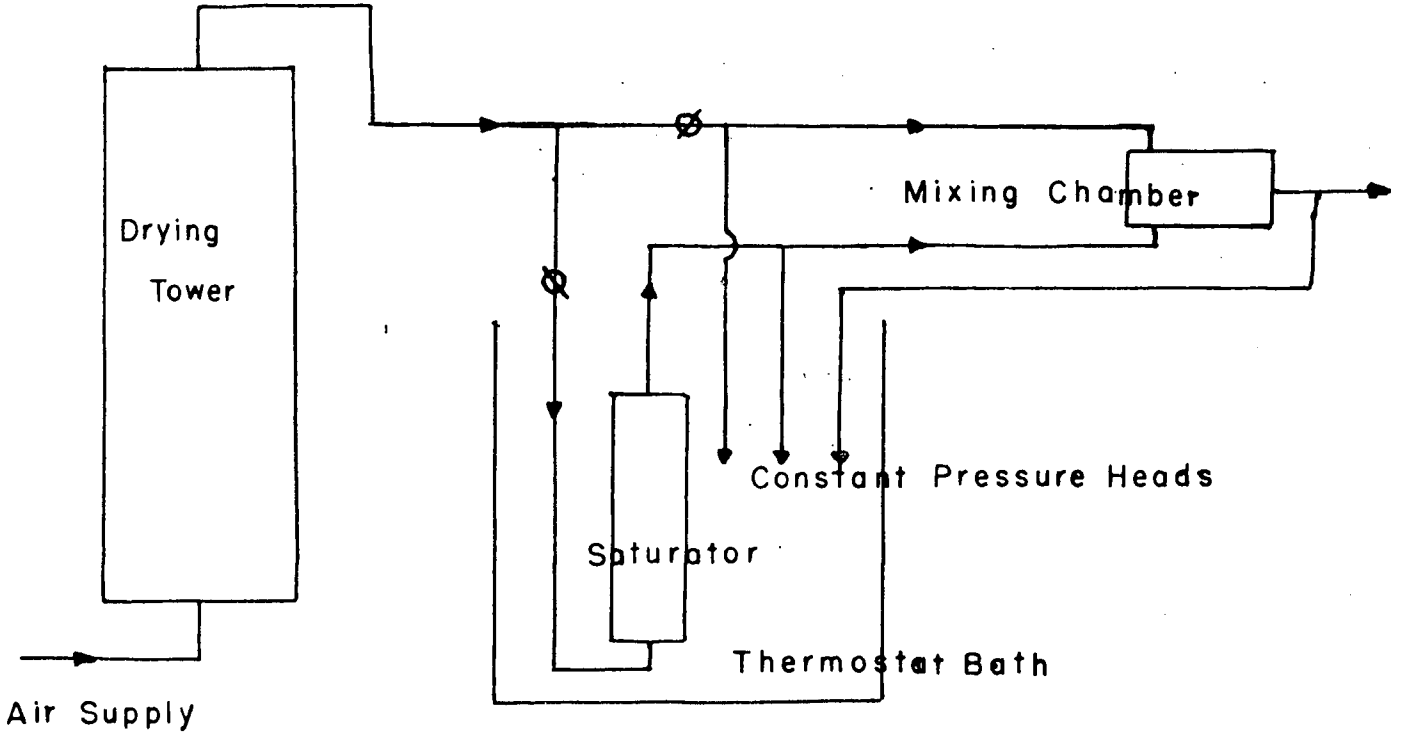

a wet-dry bulb hygrometer measures the relative humidity. The apparatus is designed to handle about 4 cubic feet per minute, an amount sufficient to change the air in the cabinet once every minute.

The behaviour of a material at any one frequency in forced vibrations may be described by a single Voigt unit with parameters E and η, whose equation of motion for forced vibration under an harmonic applied force $F = F_{max} \cos \omega t$ is:

$$M\ddot{x} + \frac{2A}{l}\eta\dot{x} + \frac{2A}{l}E = F_{max} \cos \omega t \qquad (1)$$

if no frictional resistance or elastic reaction is offered by the mechanical parts of the vibrator itself. Since the leads and supports and air friction result in some dissipative resistance, $R_1 \frac{dx}{dt}$, and since the spring part of the leads and the pendulum action of the oscillator unit provide an elastic reaction, $P_1 x$, equation (1) may be rewritten as:

$$M\ddot{x} + R\dot{x} + Px = F_{max} \cos \omega t \qquad (2)$$

where $R = \frac{2A}{l}\eta + R_1$ (3); $P = \frac{2A}{l}E + P_1$ (4)

It is difficult to verify the assumption that the dissipative resistance is proportional to the velocity of the moving unit. The factor 2 takes account of the fact that there are two lengths of fiber in the apparatus. Since the moving parts do not all have the same acceleration, M here refers to the effective mass of the system and is not equal to the sum of the masses of the

various components of the unit.

If Equation (2) is to be valid for any material over a range of frequencies, E and η must be considered as parameters which are frequency dependent. Since the variables of equation are x and t, a steady state solution is given by:

$$x = \alpha' \cos \omega t + \beta' \sin \omega t \qquad (5)$$

where

$$\alpha' = \frac{F_{max}\,(M\omega^2 - P)}{(M\omega^2 - P)^2 + R^2\omega^2} \qquad (6)$$

and

$$\beta' = \frac{F_{max}\,R\omega}{(M\omega^2 - P)^2 + R^2\omega^2} \qquad (7)$$

Differentiation of (5) with respect to time and use of (6) and (7) shows that the displacement amplitude is

$$x_{max} = F_{max}\left[(M\omega^2 - P)^2 + R^2\omega^2\right]^{-\frac{1}{2}} \qquad (8)$$

In most of this work the condition of mechanical resonance, i.e. when (x_{max}/F_{max}) is a maximum, was found by frequency tuning. The amplitude to impressed force ratio at resonance is found analytically by differentiating (8) with respect to ω. Such an operation requires that one consider the dependence of P and R on frequency. The work of Dillon et al [26] suggests that one assumes $\eta\omega$ be equal to a constant, and hence for R_i negligible, that $R\omega$ be put equal to a constant. Also, since Dillon's work indicates that E is largely independent of ω, P is set equal to a constant. With these assumptions one finds that the resonance condition $\frac{\partial}{\partial\omega}\left(\frac{x_{max}}{F_{max}}\right) = 0$ is satisfied if $M\omega^2 = P$ and this

in turn, gives, from (8)

$$x_{max} = \frac{F_{max}}{R\omega}$$

Thus, the parameters E and η are given by

$$P = \frac{2A}{l} E + P_1 = M\omega^2 \qquad (9)$$

and:

$$R = \frac{2A}{l} \eta + R_1 = \left(\frac{F_{max}}{x_{max}\,\omega}\right)_r \qquad (10)$$

subject to the assumption that $\eta\omega$ = constant and $E \neq E(\omega)$ Determination of these parameters for all fibers studies by Dunell and Dillon [25], using these equations, showed $\eta\omega$ = constant and E = constant and supported the validity of obtaining the parameters by this method. The method of mass tuning, as shown by these workers, gives the same values to the parameters but is very tedious.

2. Calibration of the Solenoids and Mass Determination

The two solenoids, or vibrator units, constructed were calibrated so that the force they exert can be determined from the current that is put through them. To do this, the whole apparatus was set up vertically and the solenoid suspended in the magnetic field from a linear spring of accurately known modulus. The vibrator and spring were then loaded with a succession of analytical weights, the vibrator being brought back to approximately its original unloaded position by passing a direct current through the coil in the appropriate direction. The current and the distance between the loaded and unloaded

positions were recorded. The force which the current exerts is given by

$$F = Mg + k\Delta x$$

where M the loading mass, g the gravitational constant, k the modulus of the spring and Δx the distance between the loaded and unloaded positions. The plot of F against I gives a straight line of slope γ dynes/ma. An alternating current whose root-mean-square value, read on the A.C. ammeter, is I exerts a maximum force of $\sqrt{2}\,\gamma I$. The calibration curves for units 1 and 2, windings a, b and c, are shown in Figures 15, 16, 17, 20, 21 and 22.

The effective mass of the system may be determined from vibrational data when the solenoids have been calibrated. In Equation (8), $R\omega$ is negligible compared to $M\omega^2 - P$ for values of ω which are not too close to ω_r . Hence a plot of $\pm \frac{F_{max}}{x_{max}}$ against ω^2 for any material tested should yield a curve which deviates from a straight line only near resonance, the slope being M, the effective mass of the system. Nylon filaments were placed in the vibrator and values of F_{max} and x_{max} obtained for a series of frequencies on either side of resonance. Figures 18, 23 and 24 give plots of (F_{max}/x_{max}) against ω^2 for windings 1a, 2a and 2b. The fact that the effective mass obtained from 2a and 2b did not agree led to the following method of re-evaluating both the coil calibration and the effective mass of unit No. 2.

Assuming the coil calibration to be in error, let F'_{max} be the force corresponding to a current I according to the D.C.

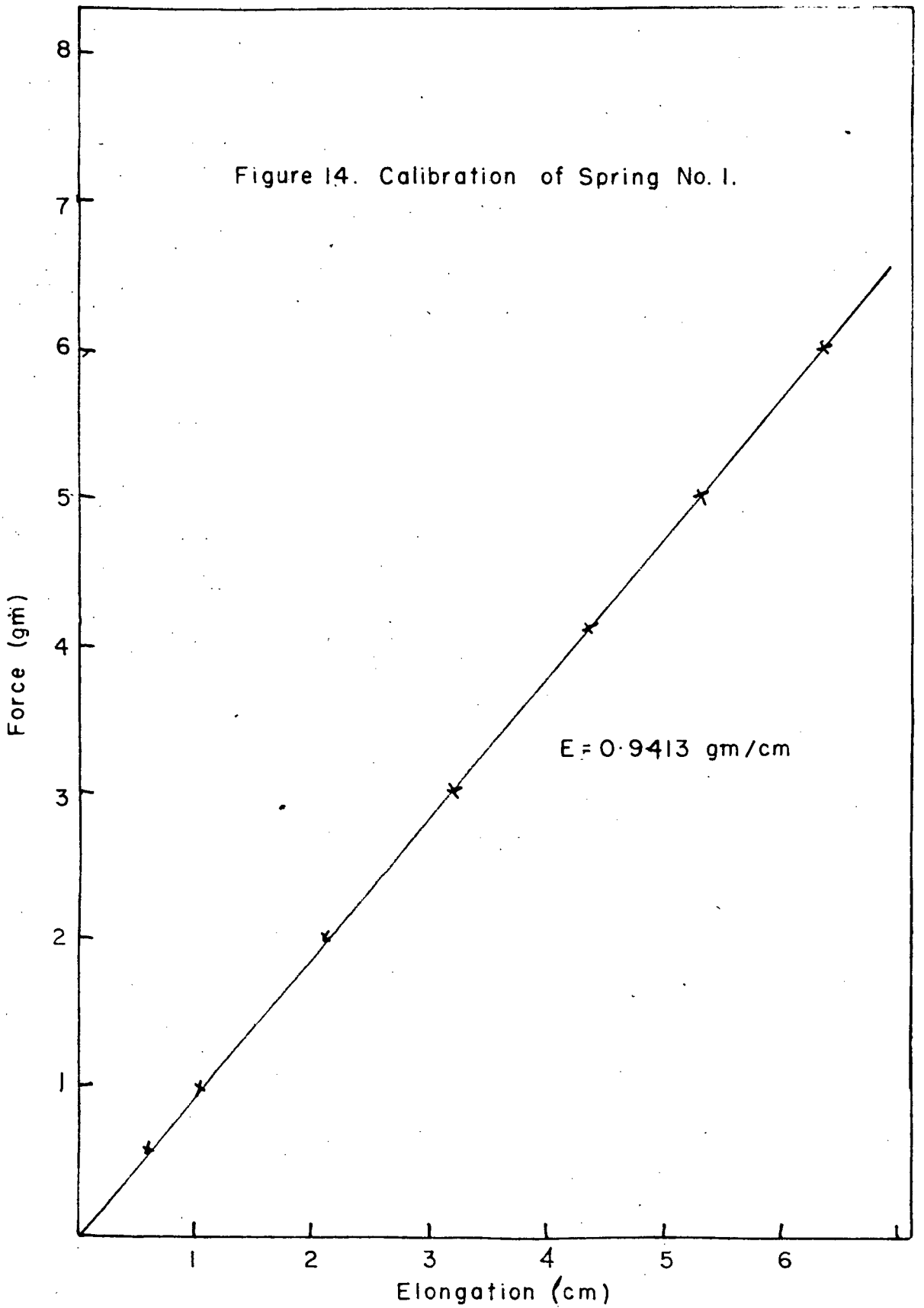

Figure 14. Calibration of Spring No. I.

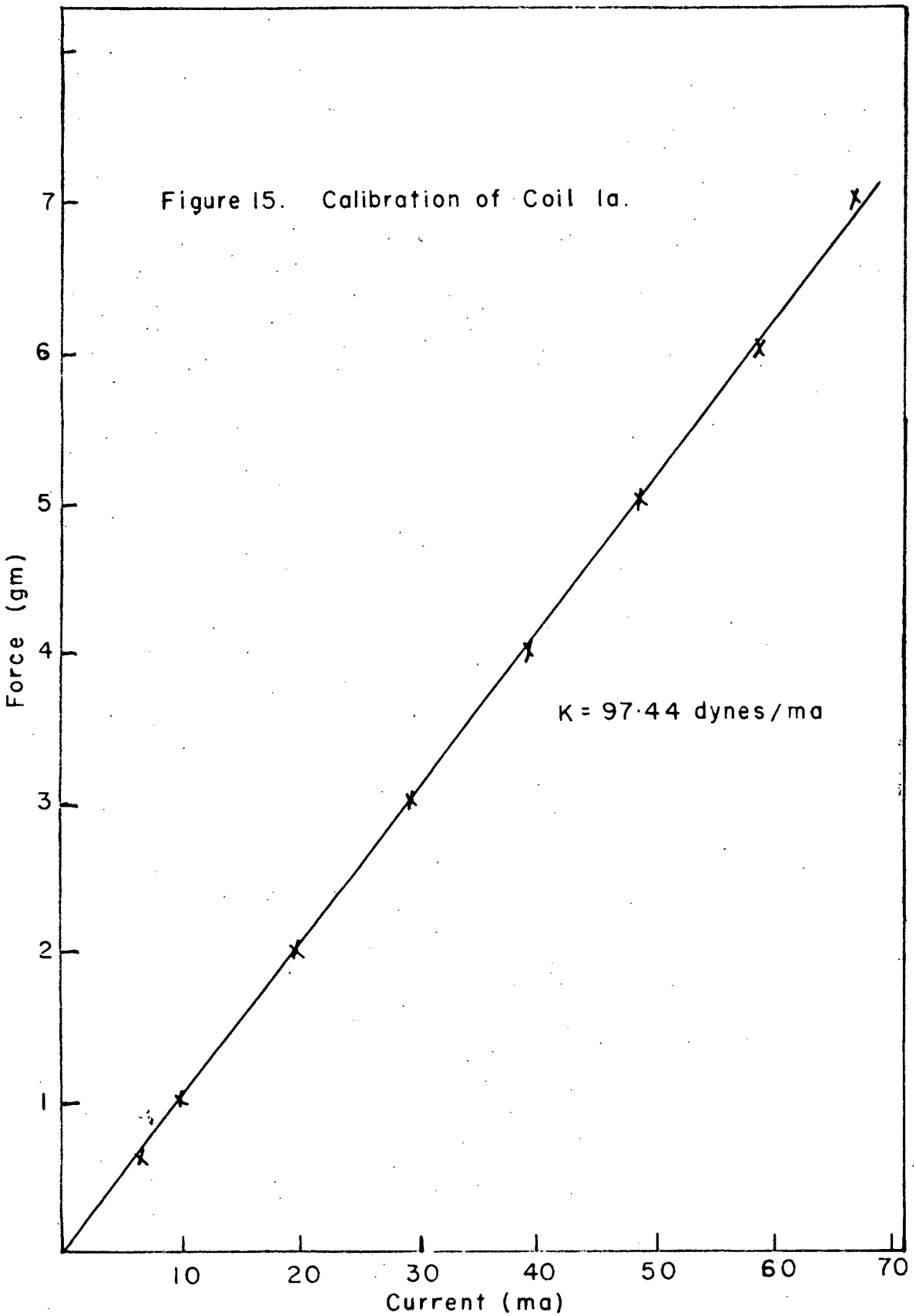

Figure 15. Calibration of Coil Ia.

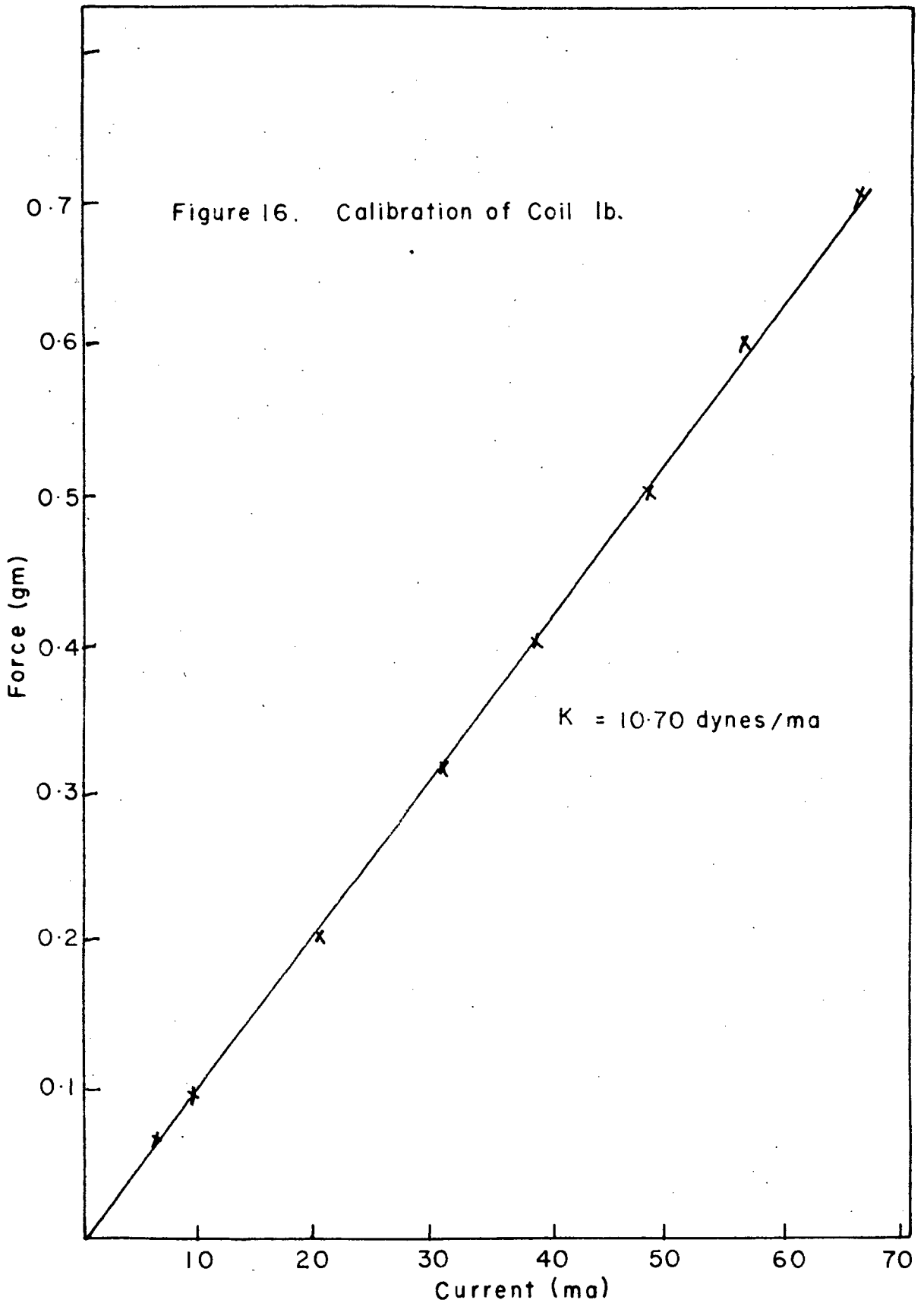
Figure 16. Calibration of Coil Ib.
0·7
0·6
0·5
0·4
0·3
0·2
0·1
Force (gm)
K = 10·70 dynes/ma
10
20
30
40
50
60
70
Current (ma)

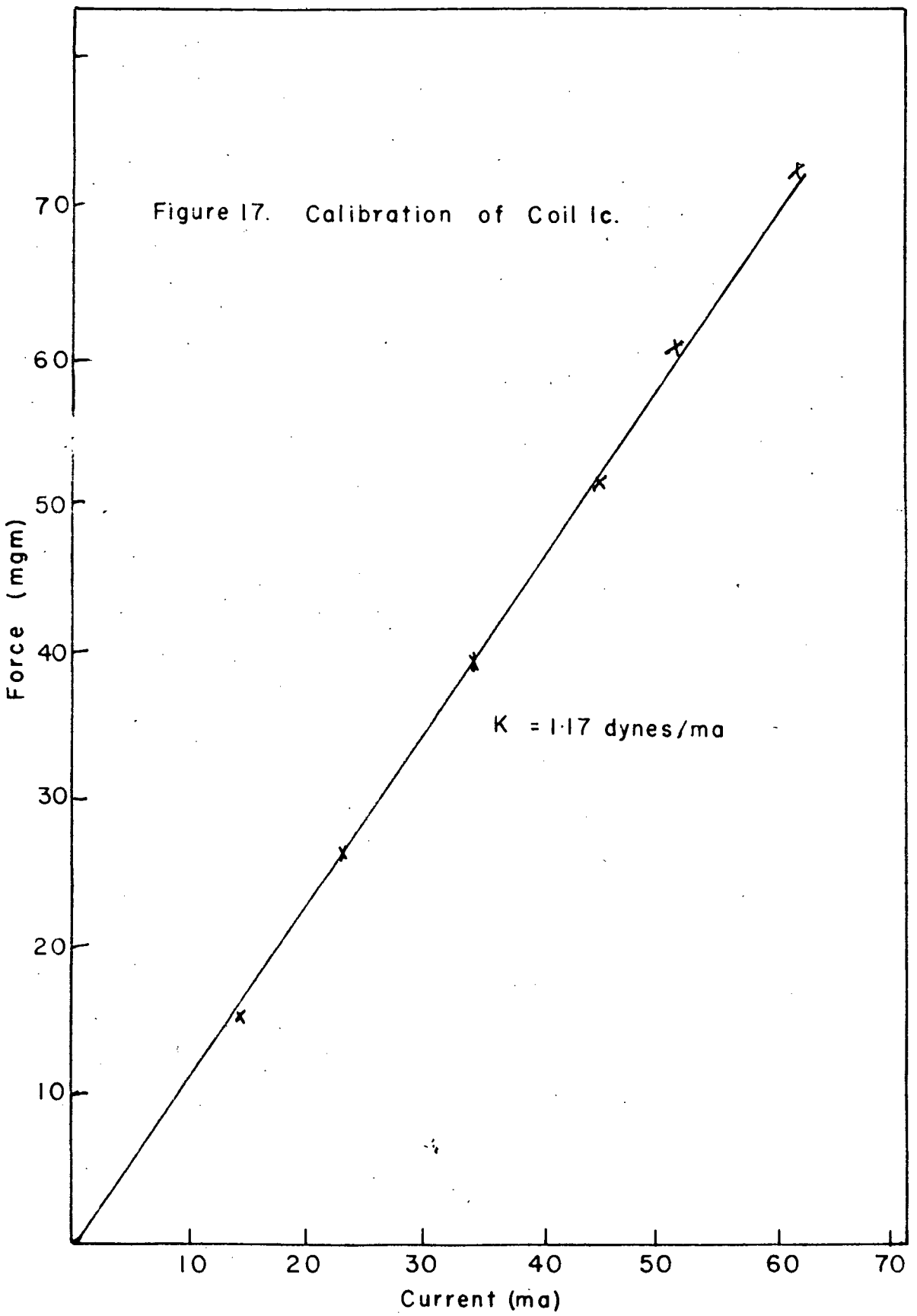
Figure 17. Calibration of Coil Ic.
Force (mgm)
Current (ma)
K = 1·17 dynes/ma
10
20
30
40
50
60
70

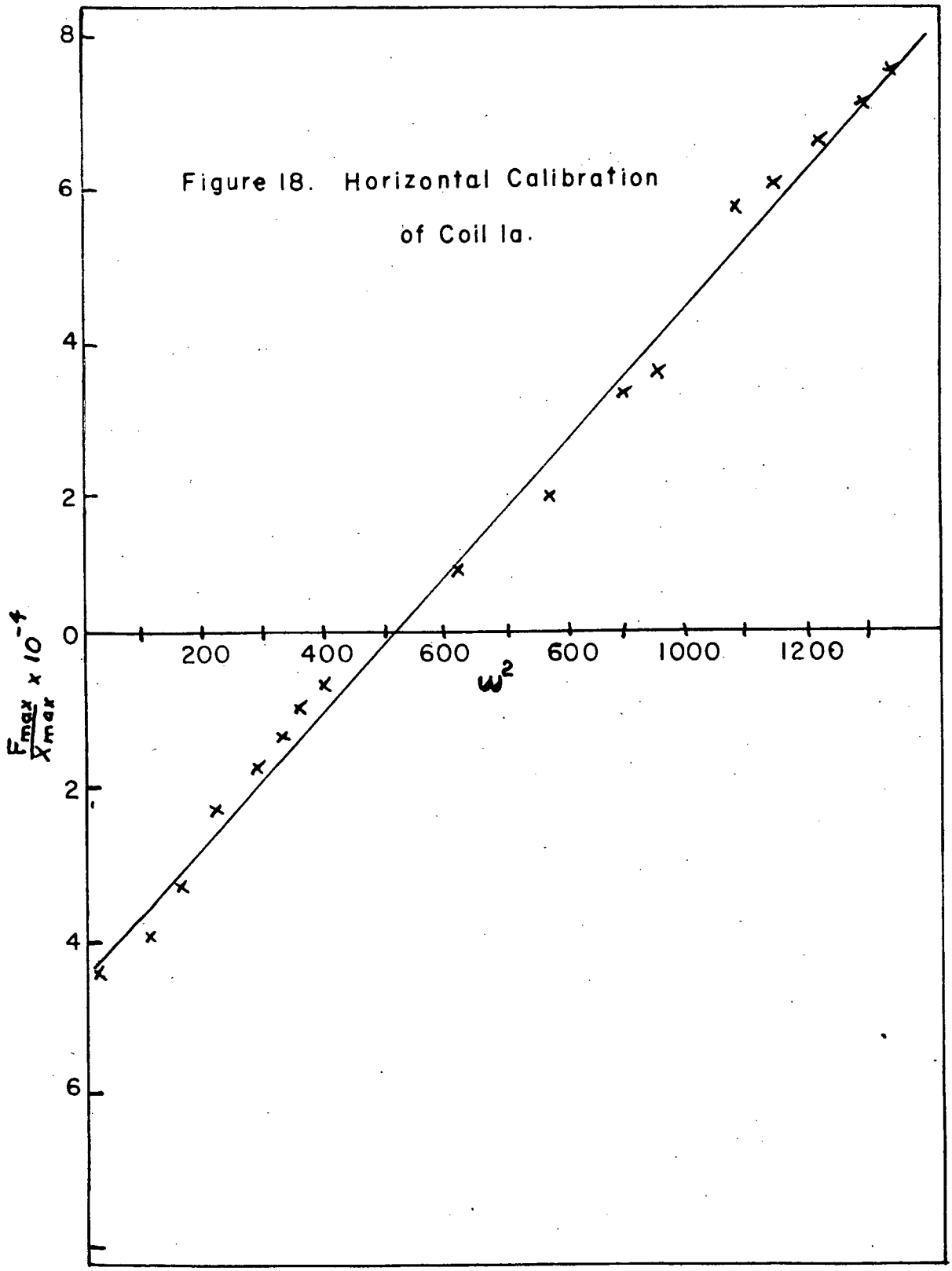

Figure 18. Horizontal Calibration of Coil Ia.

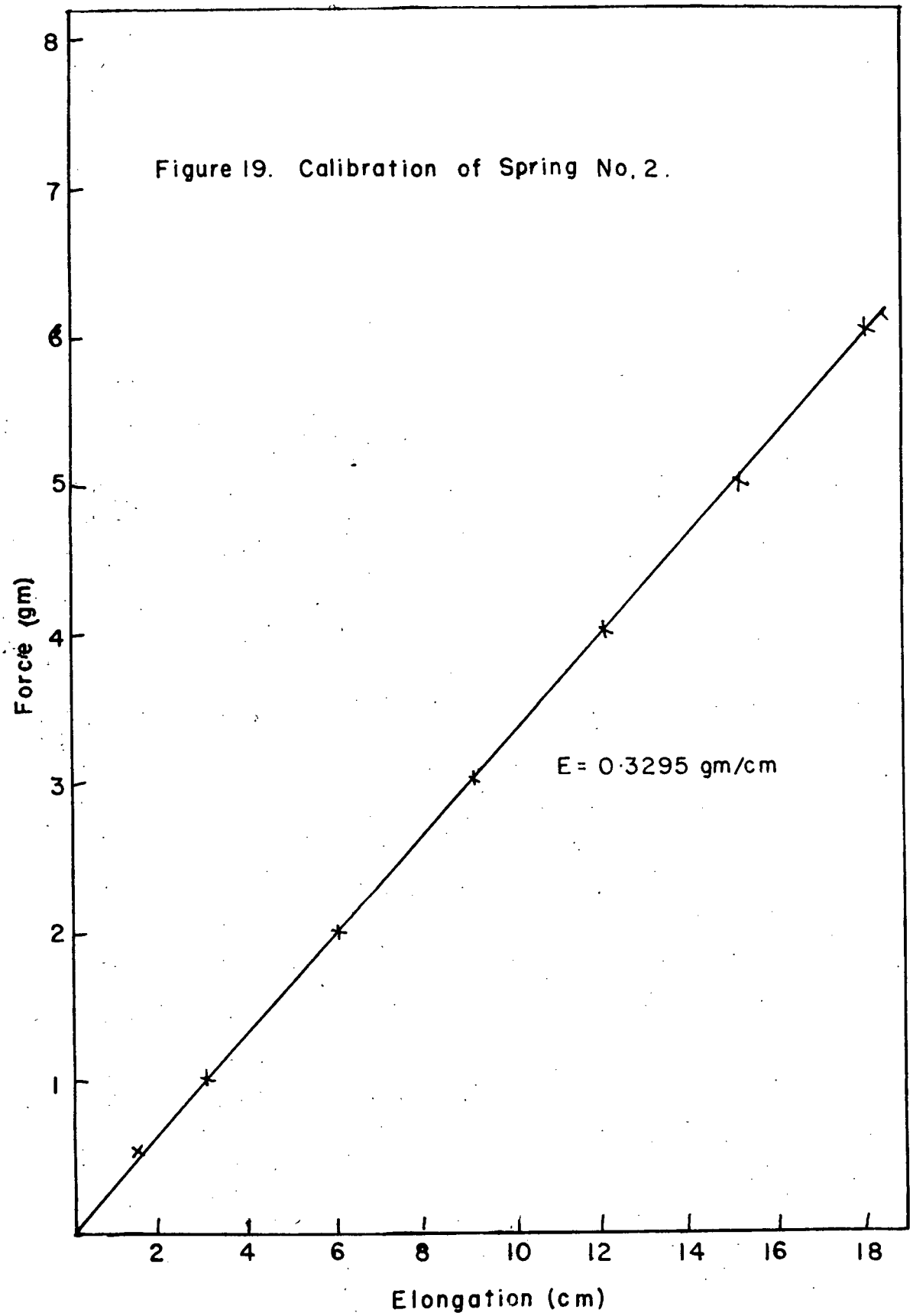

Figure 19. Calibration of Spring No. 2.

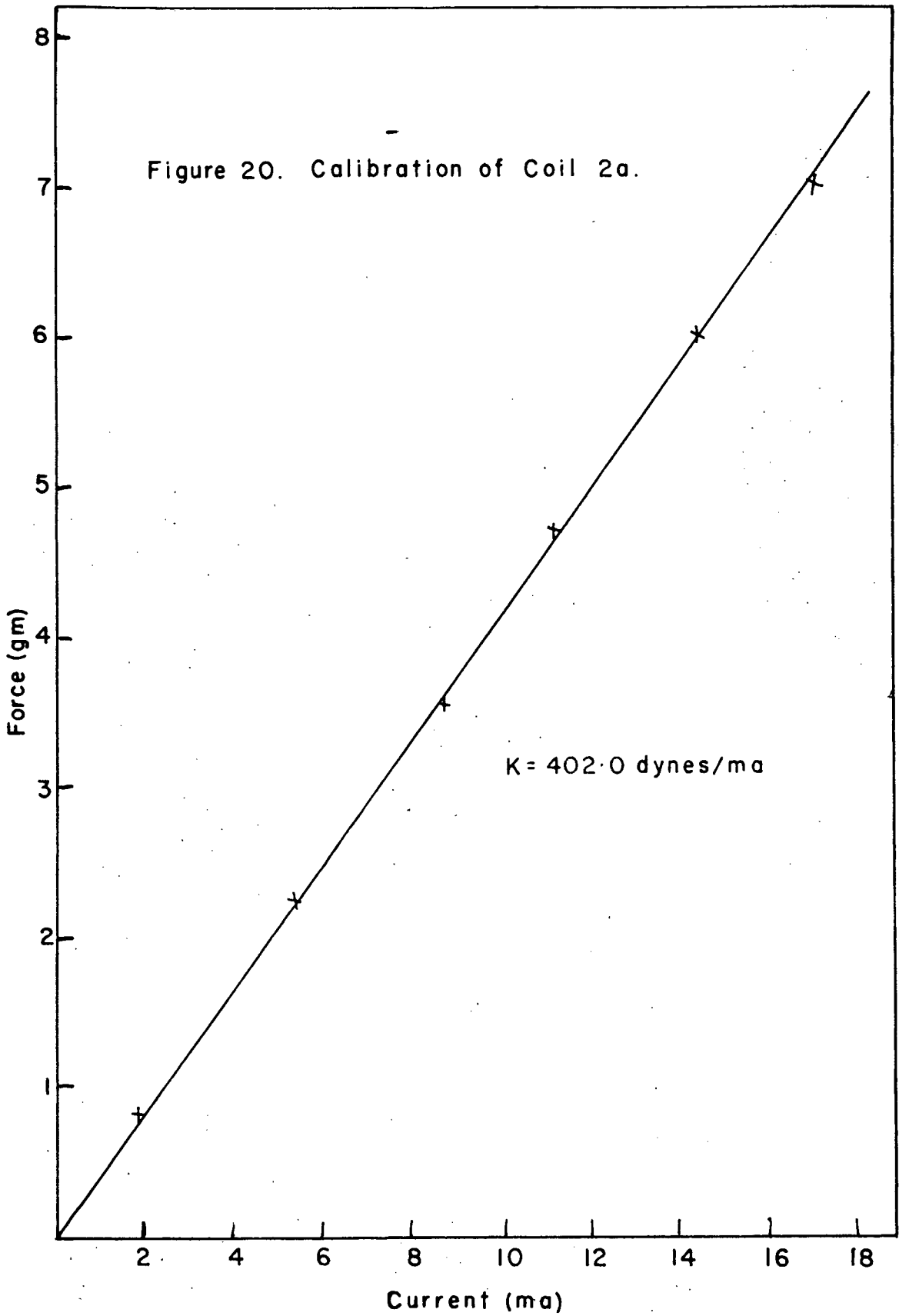

Figure 20. Calibration of Coil 2a.

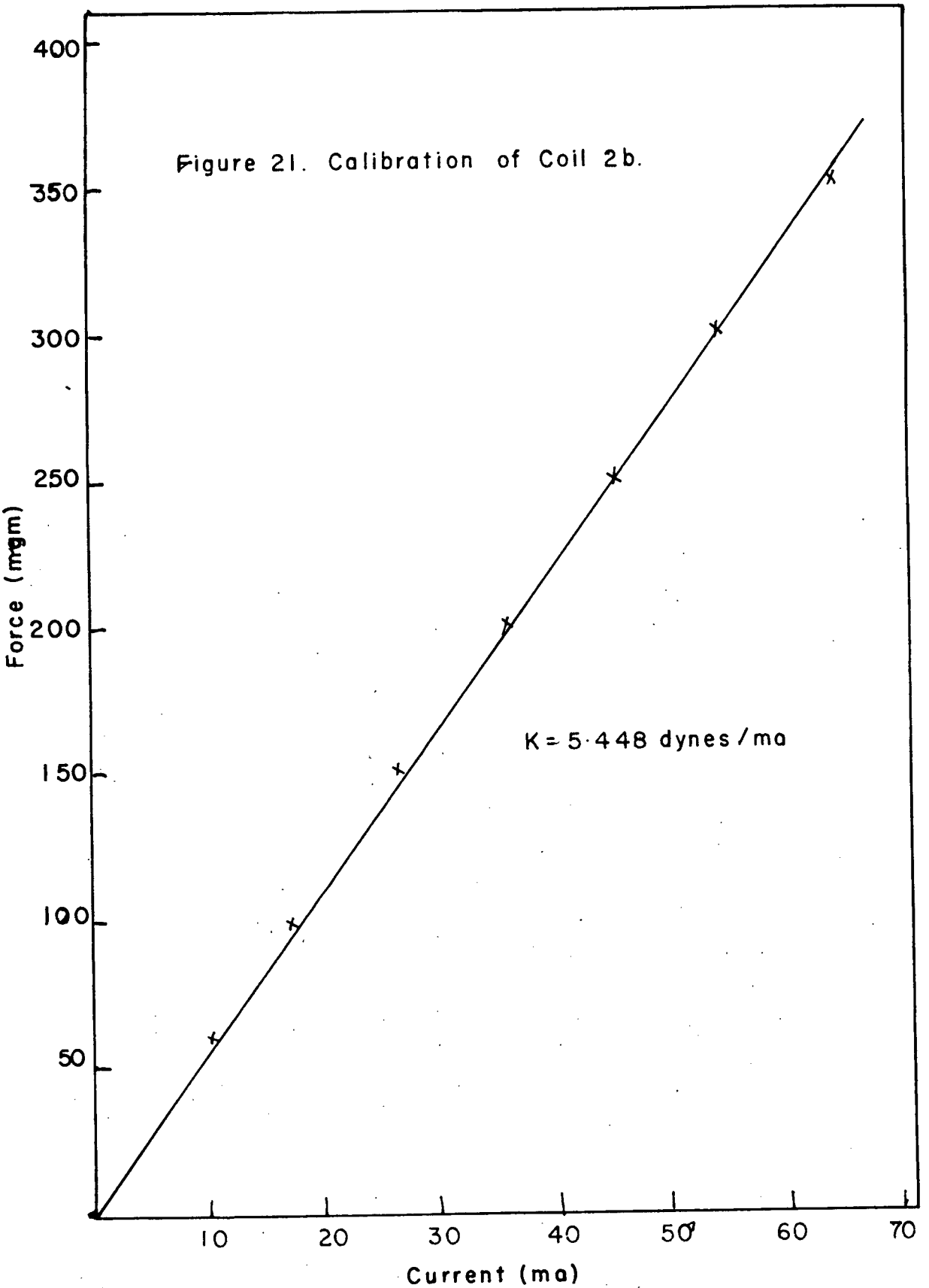
Figure 21. Calibration of Coil 2b.
400
350
300
250
200
150
100
50
Force (mgm)
K = 5·448 dynes / ma
10
20
30
40
50
60
70
Current (ma)

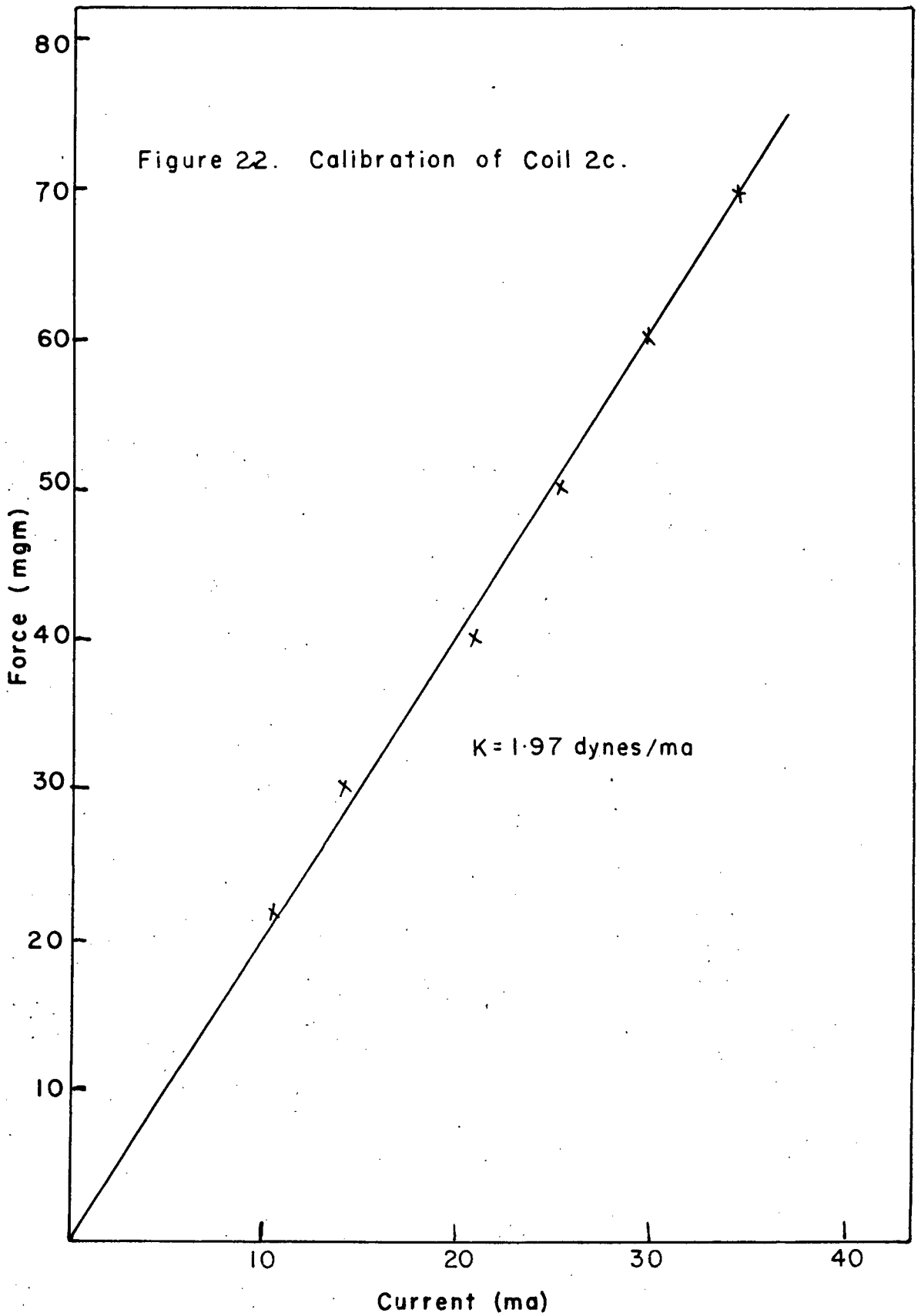
Figure 22. Calibration of Coil 2c.
80
70
60
50
40
30
20
10
Force (mgm)
K = 1·97 dynes/ma
10
20
30
40
Current (ma)

calibration, and let F_{max} be the true force corresponding to the current **I**. Now:

$$F'_{max} = P F_{max}$$

Let M' be the apparent mass of the system determined on the basis of F' values, and let M be the true mass. Using the vibrational data obtained we have:

$$\left(\frac{F'_{max}}{x_{max}}\right)_1 = P\left(\frac{F_{max}}{x_{max}}\right)_1 \cong M'\omega_1^2 - P$$

and:

$$\left(\frac{F'_{max}}{x_{max}}\right)_2 = P\left(\frac{F_{max}}{x_{max}}\right)_2 \cong M'\omega_2^2 - P$$

sufficiently far from resonance that $R^2\omega^2$ may be neglected. From these two equations:

$$\left(\frac{F'_{max}}{x_{max}}\right)_2 - \left(\frac{F'_{max}}{x_{max}}\right)_1 = P\left[\left(\frac{F_{max}}{x_{max}}\right)_2 - \left(\frac{F_{max}}{x_{max}}\right)_1\right]$$
$$= M'(\omega_2^2 - \omega_1^2)$$

Now:

$$M = \frac{\left(\frac{F_{max}}{x_{max}}\right)_2 - \left(\frac{F_{max}}{x_{max}}\right)_1}{(\omega_2^2 - \omega_1^2)} = \frac{M'}{P}$$

Next a known mass M_1 is added to the unit and the experiment repeated. Then we have:

$$M + M_1 = \frac{(M+M_1)'}{P}\ ;\quad \frac{M'}{P} + M_1 = \frac{(M+M_1)'}{P}\ ;\quad P = \frac{(M+M_1)' - M'}{M_1}$$

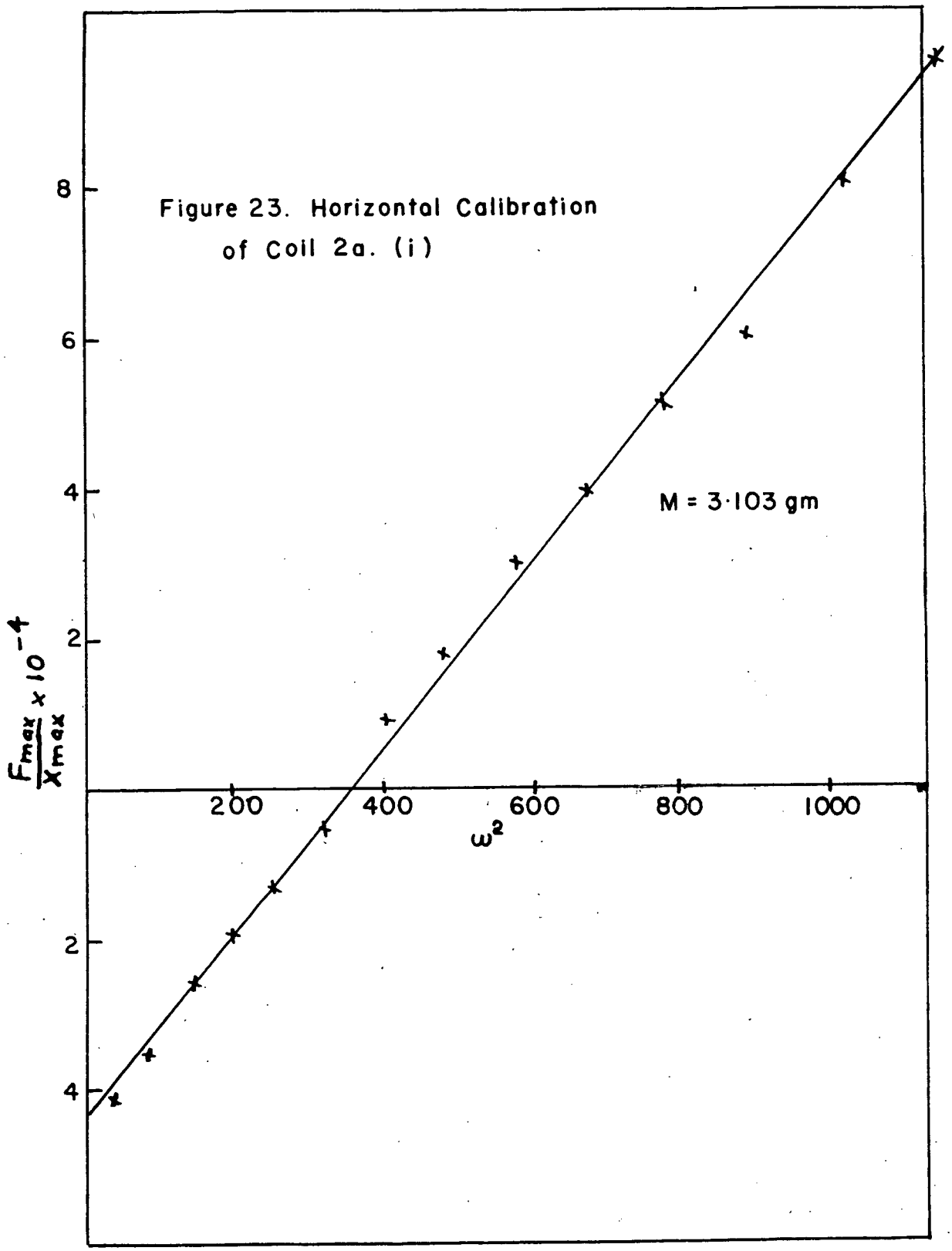

Figure 23. Horizontal Calibration of Coil 2a. (i)

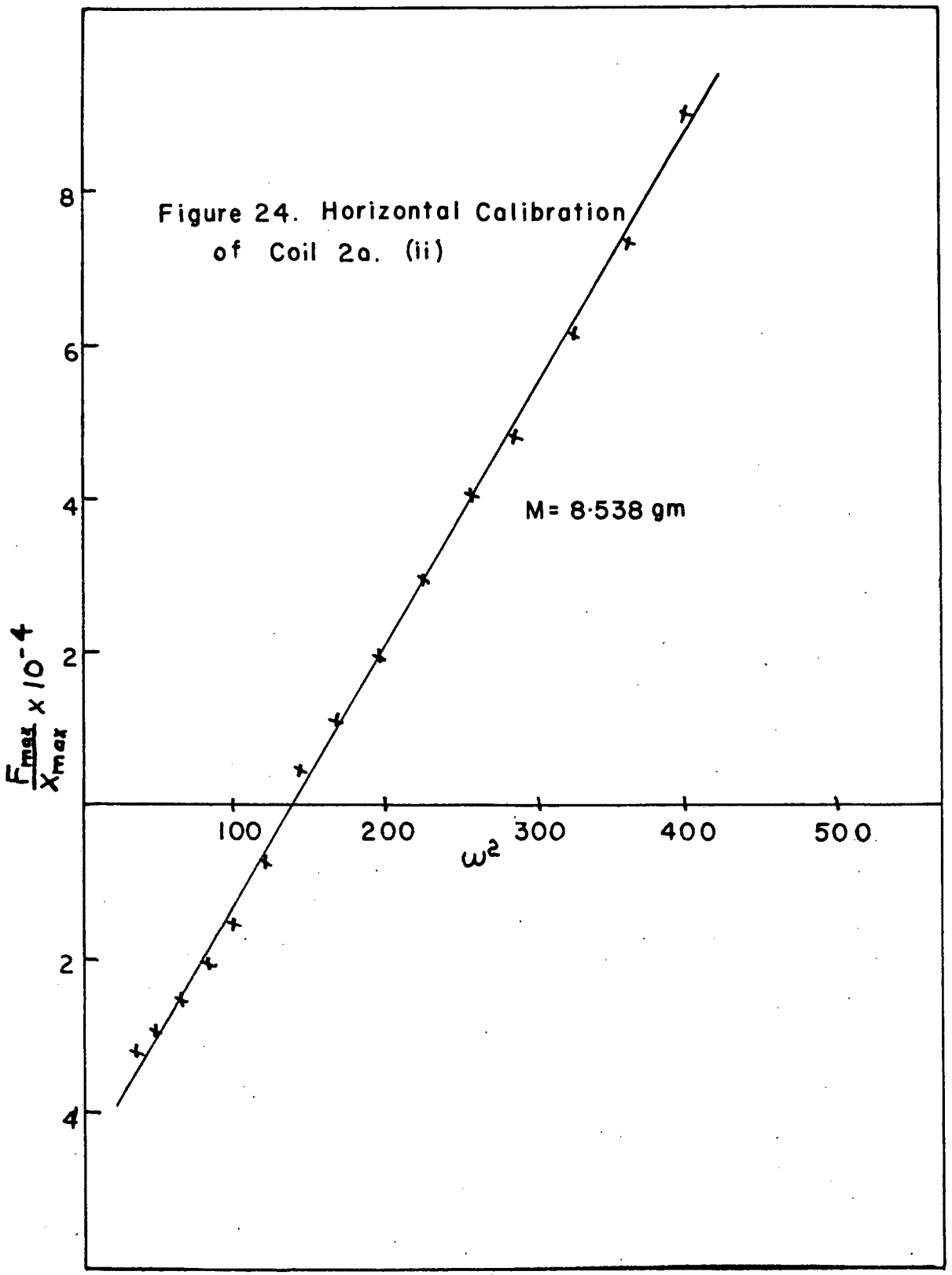
Figure 24. Horizontal Calibration of Coil 2a. (ii)
M= 8·538 gm
$\frac{F_{max}}{X_{max}} \times 10^{-4}$
ω^2
8
6
4
2
2
4
100
200
300
400
500

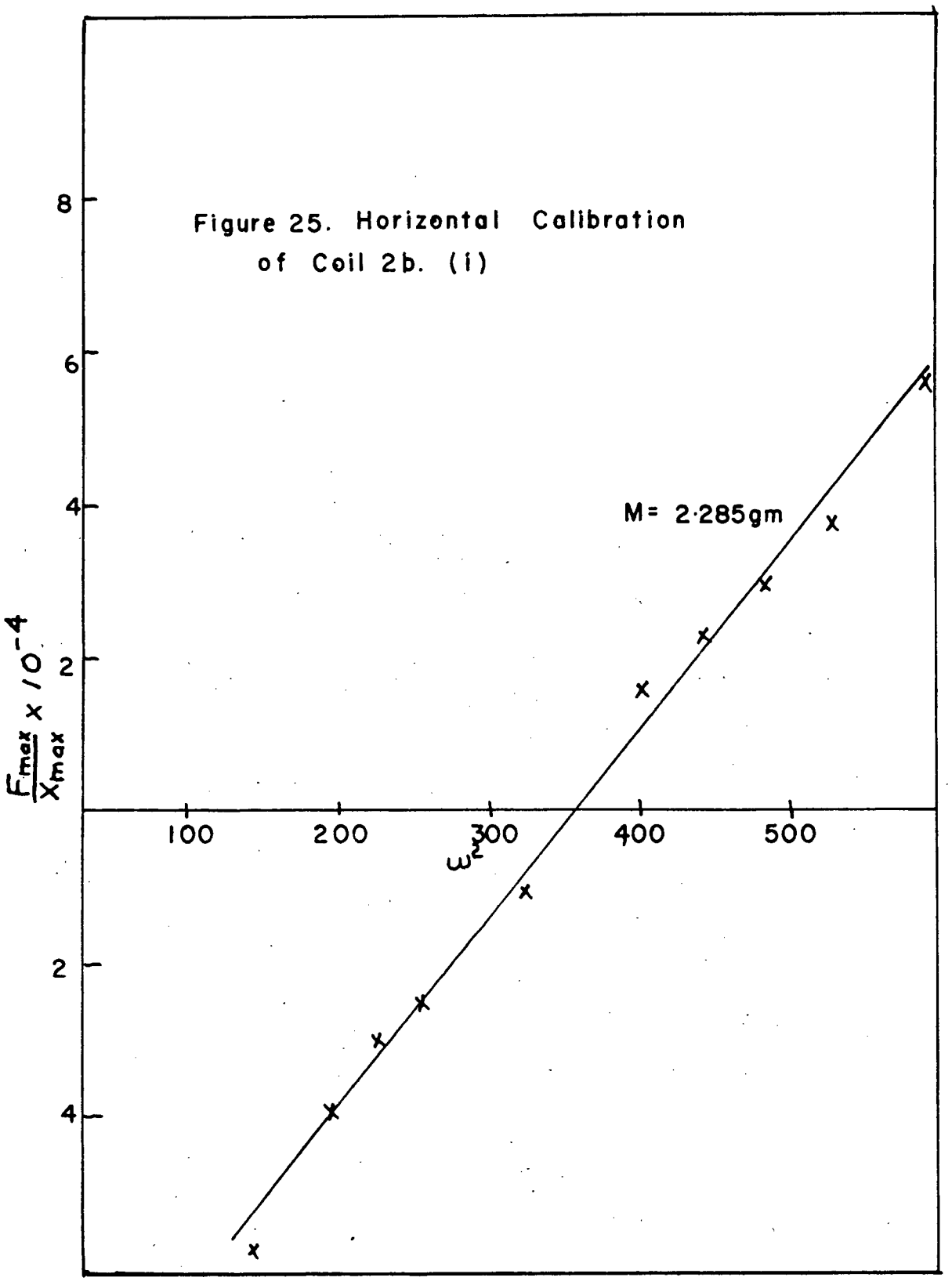
Figure 25. Horizontal Calibration
of Coil 2b. (i)
M= 2·285gm
$\frac{F_{max}}{X_{max}} \times 10^{-4}$
ω^2
8
6
4
2
100
200
300
400
500
2
4

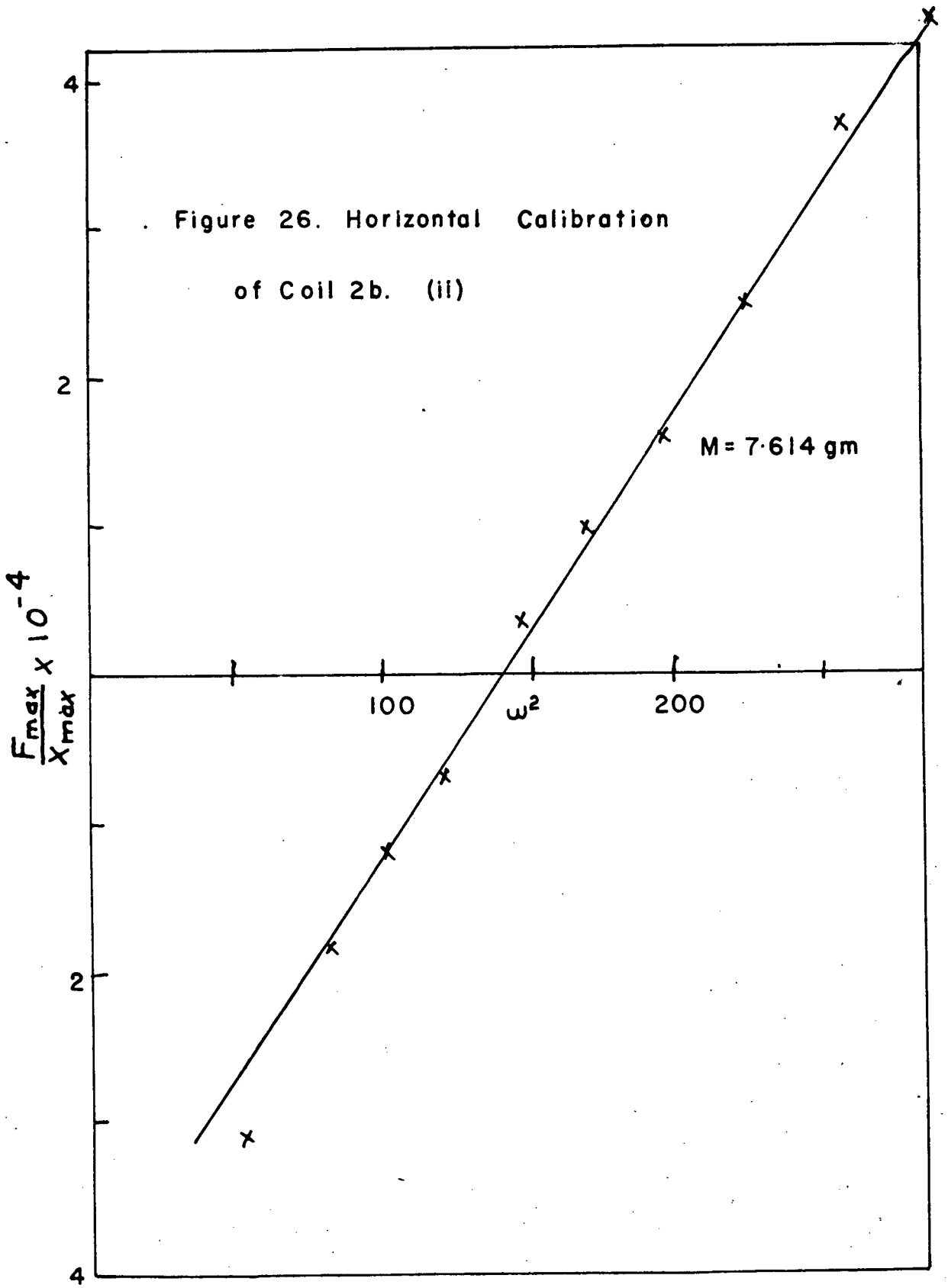

Figure 26. Horizontal Calibration of Coil 2b. (ii)

and M' and $(M+M_1)'$ are, of course, the slopes of the two experimental plots of (F_{max}/x_{max}) against ω^2. This re-calibration procedure was carried out for both windings of unit No. 2. The results are summarized in the following table.

TABLE III

	Winding a	Winding b
M'	3.103 ± 0.072	2.285 ± 0.085
M_1	5.237	5.237
$(M_1 + M)'$	8.550 ± 0.201	7.614 ± 0.266
p	1.038 ± 0.052	1.018 ± 0.067
M	2.990 ± 0.218	2.245 ± 0.209

From the two values of M in the table an average value of M was obtained:

$$M = \frac{0.209(2.990) + 0.218(2.245)}{0.218 + 0.209} = 2.516$$

Using this value of M, average values of p were obtained for each winding and corrected values of γ determined. These results are shown in Table IV, together with the γ values for winding 1a and 2c.

Unit	γ Original	p	γ Corrected
1a	1.03.7	-	-
2a	568.0	1.233	460.6
2b	7.700	0.9082	8.478
ac	1.970	-	-

Evaluation of P_1 and R_1

The elastic reaction of the coiled leads is quite negligible compared to the effect of the pendulum action of the vibrator unit. If h is the height of the suspension, then a small displacement of the unit is accompanied by a rise in height, x^2/h, of the unit and a restoring force Mgx/h acting in the same direction as the elastic reaction of the sample filaments. Thus $P_1 = Mg/h$ (See Equations (8) and (10)).

With no filaments attached to the vibrator unit the equation of motion for free vibrations is:

$$M\frac{d^2x}{dt^2} + R_1\frac{dx}{dt} + P_1 x = 0$$

from which the damping factor can be obtained from the decrease in amplitude during any n successive oscillations:

$$R_1 = \frac{M\omega}{n\pi} \ln\left[\frac{(x_{max})_n}{(x_{max})_{m+n}}\right]$$

Very little precision is attainable in the determination of R_1; that is, variations of ± 20% are encountered but, because of the magnitude of R_1, 6 dyne-sec/cm, the % error contribution to the filament tests is comparable to those from the other variables in the calculations.

RESULTS OF VIBRATIONAL EXPERIMENTS

Dunell and Dillon found a marked increase in dynamic modulus with time and a decrease in the energy loss factor for a filament as it creeps under a dead load. In order to compare rigorously the dynamic parameters of one fiber with those of another, the dynamic properties should be measured at a time after the application of tension to the filament such that comparable points on the creep curves for the fibers concerned are reached. Since points for comparison were not obtained, the experimental procedure was to allow the fiber to creep in position in the vibrator for 18 hours before dynamic measurements were made. After this time the change in the dynamic parameters with time is sufficiently small as to be insignificant during the time required to complete the experiment on the fiber.

The tensioning weight used for acetate rayon was 0.5 gm. per 10^{-6} cm.^{2} cross-sectional area and for albumin 0.25 gm. The temperature and relative humidity conditions of each experiment are given on the plots of the moduli and viscosities. The fibers were allowed at least 16 hours to come to equilibrium with the humidity conditions before the addition of the tensioning weights. The strain amplitude at resonance was about 0.002 in all experiments.

It was thought advisable that, before attempting to measure the dynamic parameters of the albumin fibers, tests should

be made on acetate fibers and the results compared with those obtained by Dunell and Dillon. The results of this comparison are given in Figures 27 and 30. The variation of dynamic viscosity and modulus with frequency of two egg albumin fibers of differing steam elongation (54% and 120%) are given in Figures 28 and 31. Each fiber was vibrated at the lower humidity first and then allowed to relax without tension for 24 hours before the addition of the tensioning weights for the second test at the higher humidity.

Since the variation of the dynamic parameters of egg albumin fibers is within the variation of these parameters from fiber to fiber and since the same regularity of variation with humidity was not found previously with acetate (Figure 27), it was decided to test one acetate fiber at three relative humidities. Here also, the fiber was vibrated at the lower humidity first and allowed to relax 16 hours without tension at the higher humidity before the tensioning weights were added for the next test. The results of these experiments are given in Figures 29 and 32.

Results of stress relaxation experiments by J. Pattison on acetate with varying humidity and on albumin (54) are given in Figures 33 and 34.

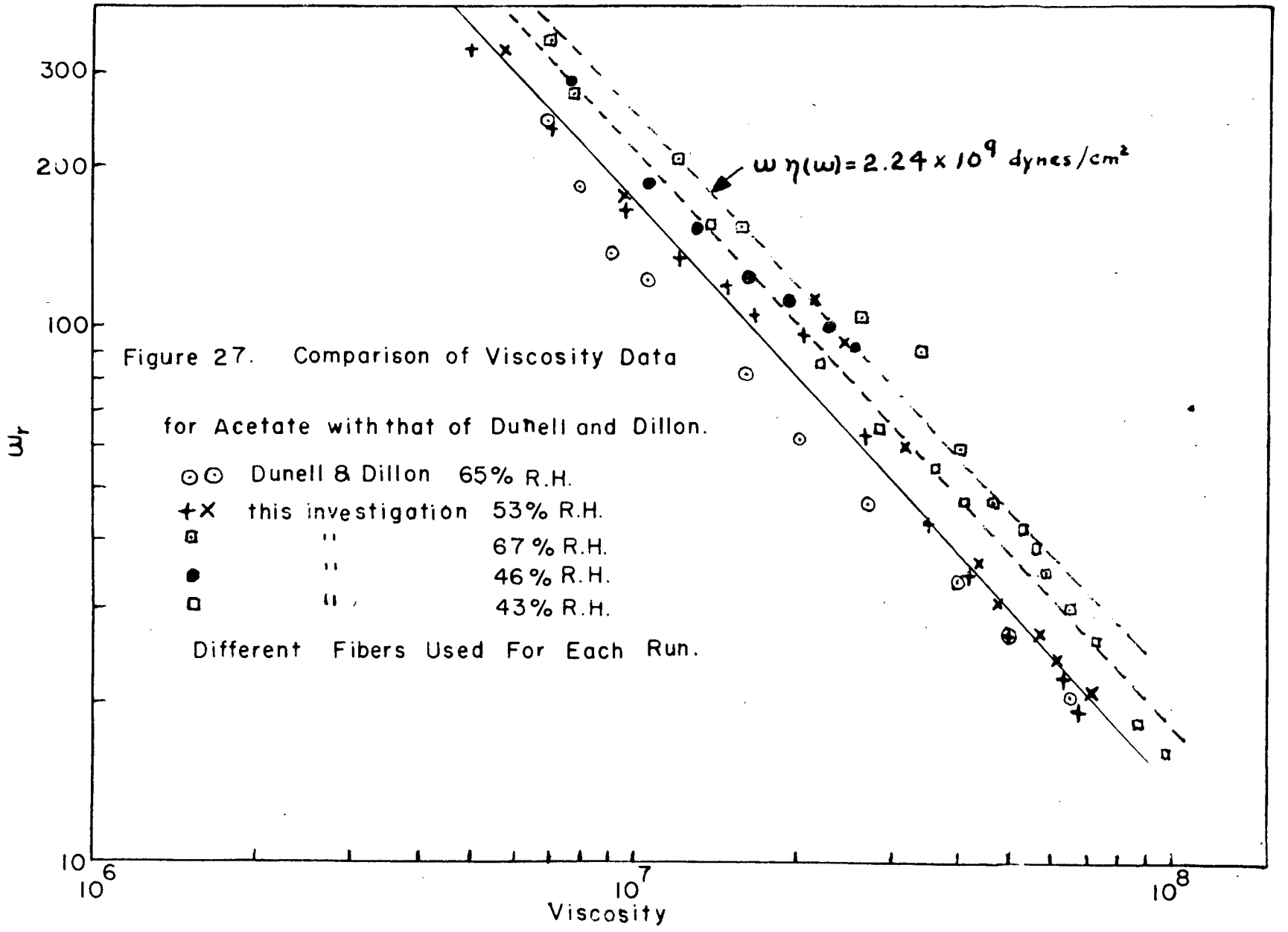
300
200
100
10
ω_r
10^6
10^7
10^8
Viscosity
$\omega\,\eta(\omega) = 2.24 \times 10^9$ dynes/cm²
Figure 27. Comparison of Viscosity Data
for Acetate with that of Dunell and Dillon.
⊙⊙ Dunell & Dillon 65% R.H.
+× this investigation 53% R.H.
⊡ " 67% R.H.
● " 46% R.H.
□ " 43% R.H.
Different Fibers Used For Each Run.

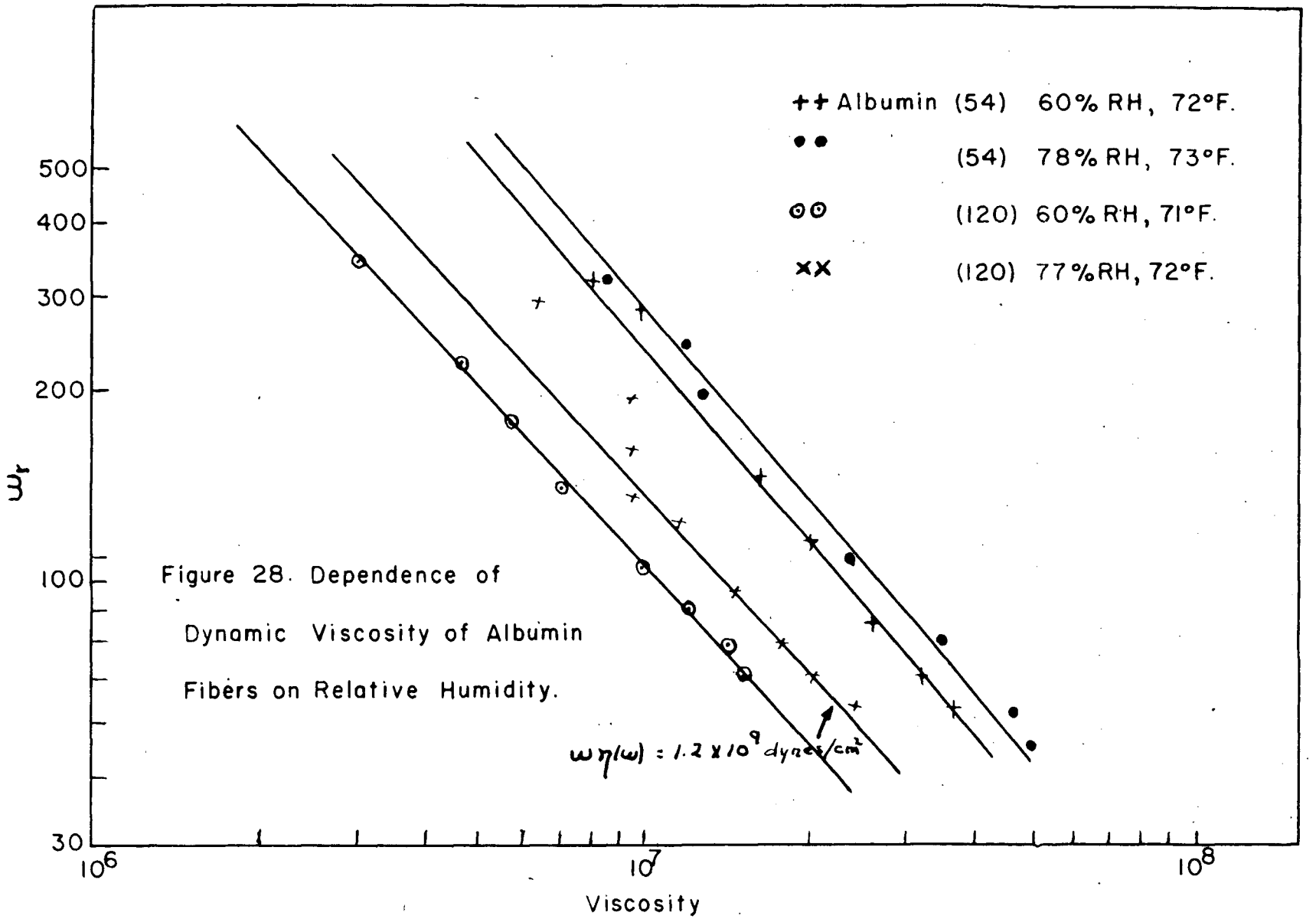

Figure 28. Dependence of Dynamic Viscosity of Albumin Fibers on Relative Humidity.

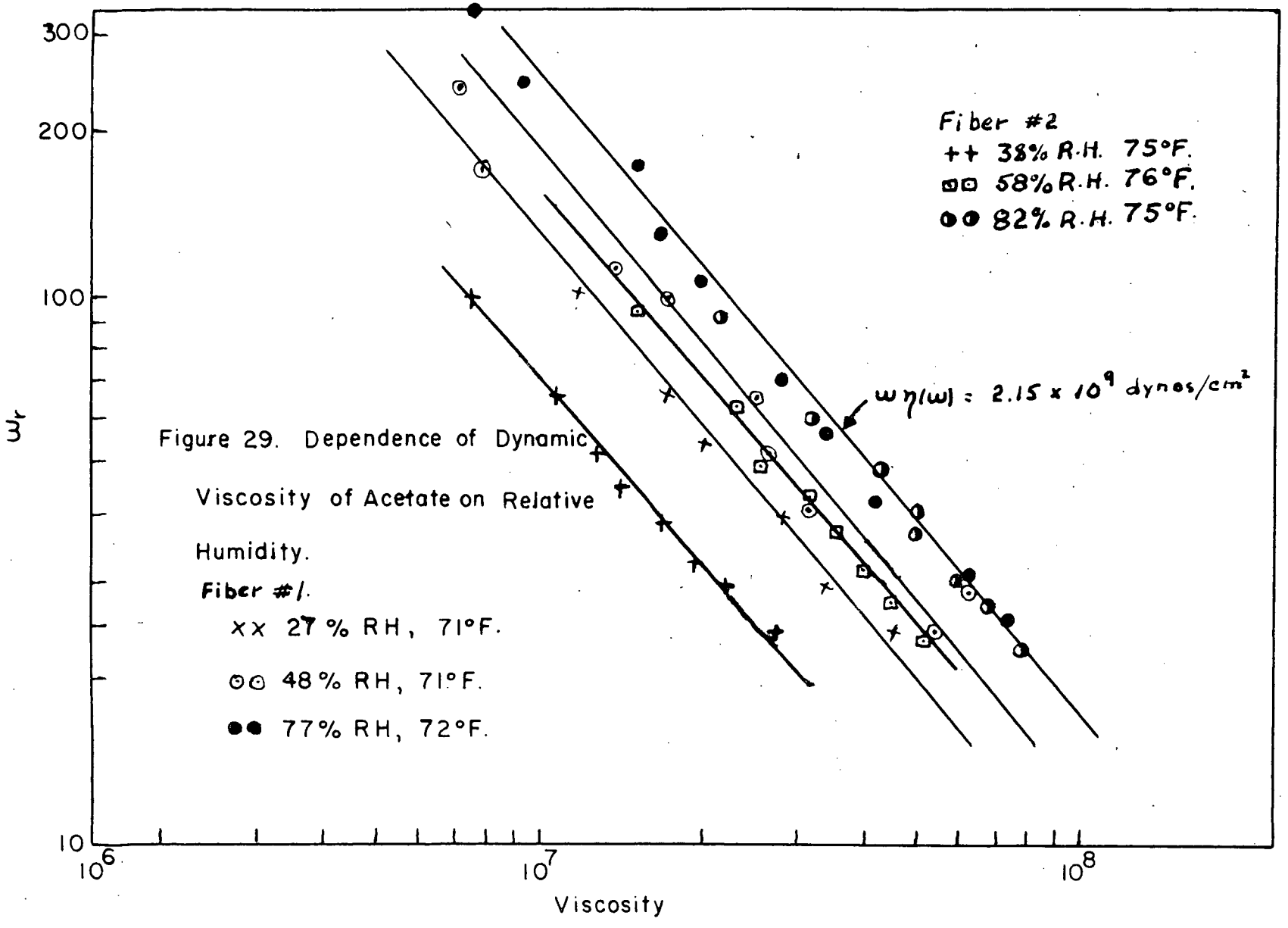

Figure 29. Dependence of Dynamic Viscosity of Acetate on Relative Humidity.

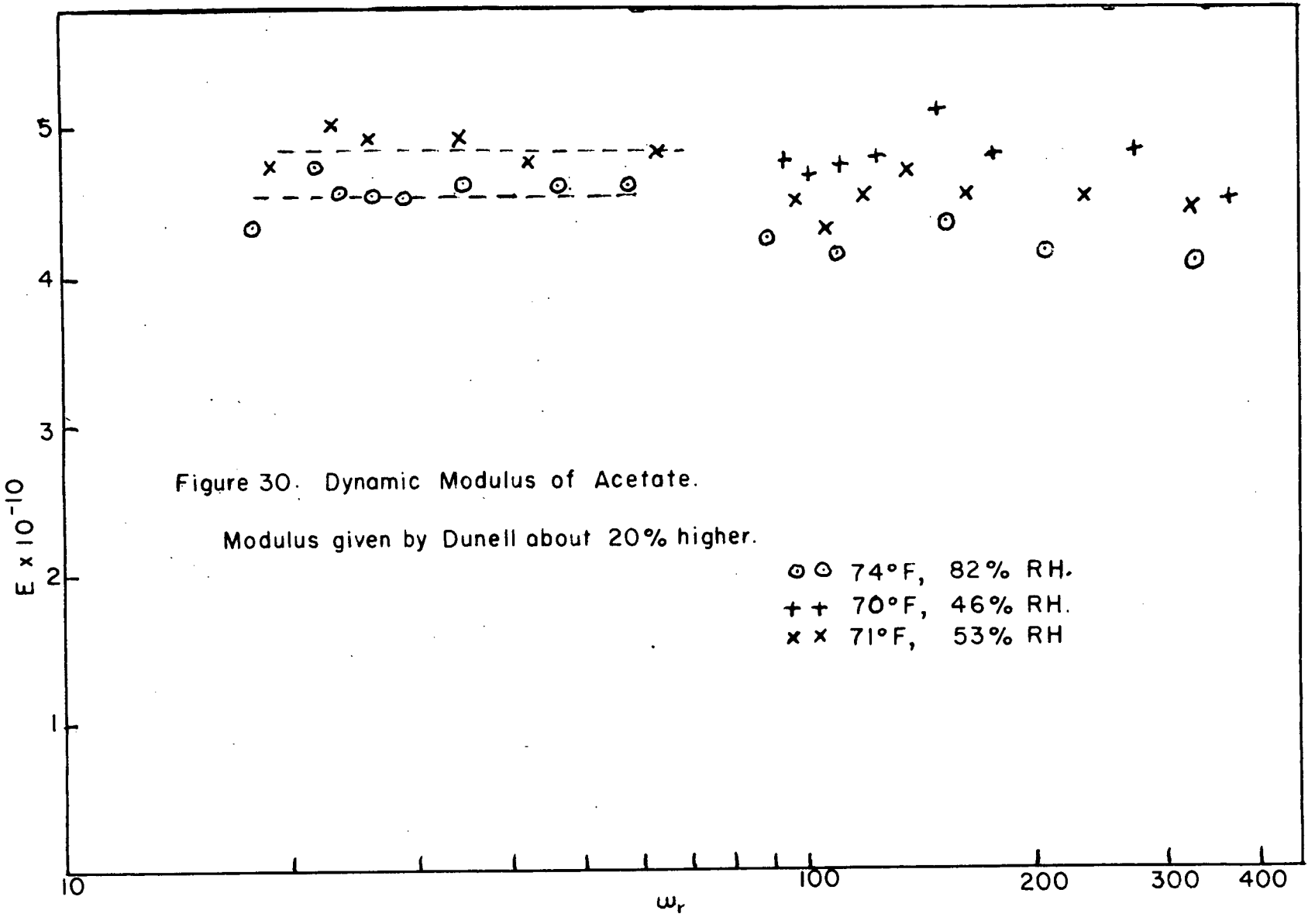

Figure 30. Dynamic Modulus of Acetate.

Modulus given by Dunell about 20% higher.

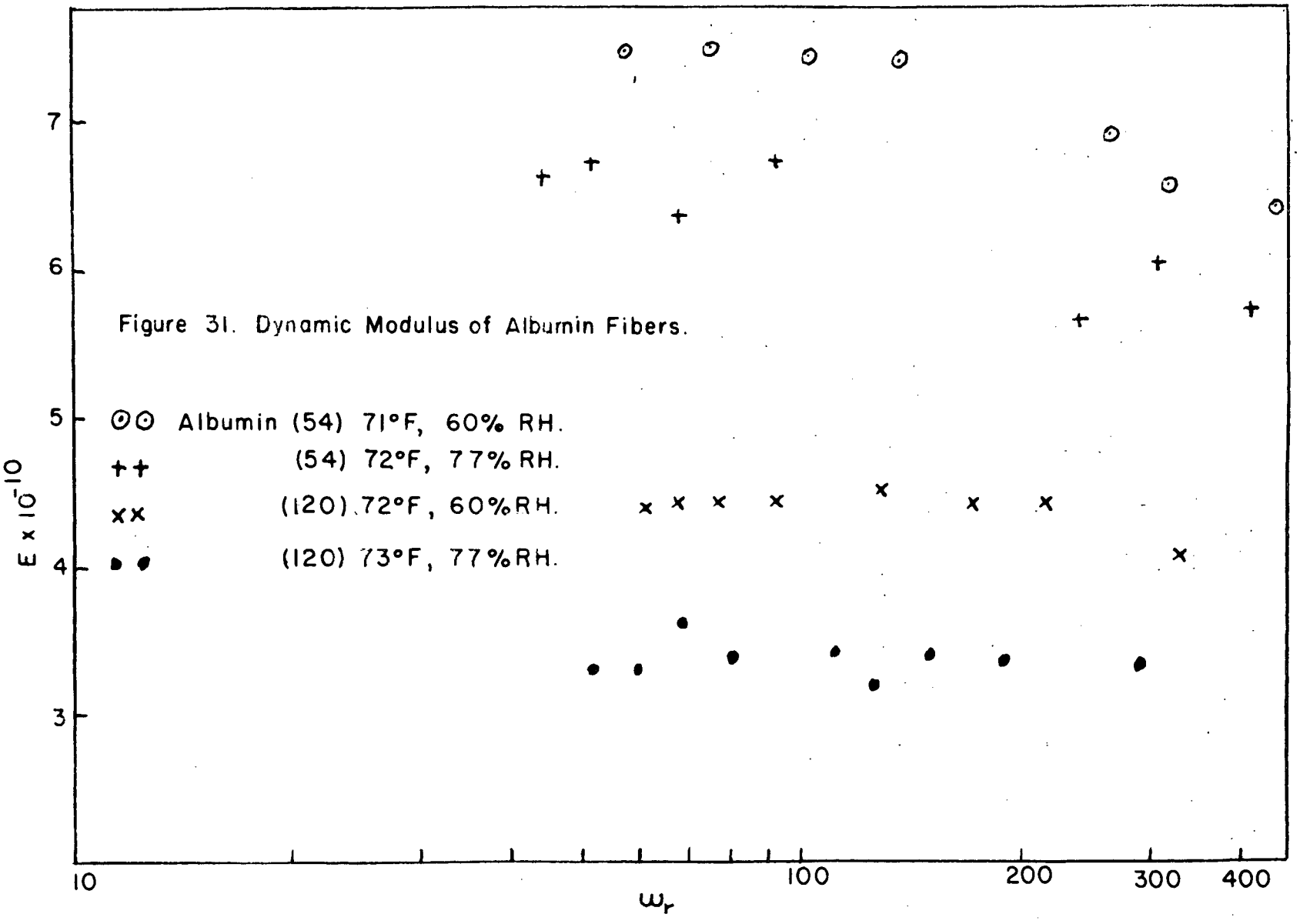

Figure 31. Dynamic Modulus of Albumin Fibers.

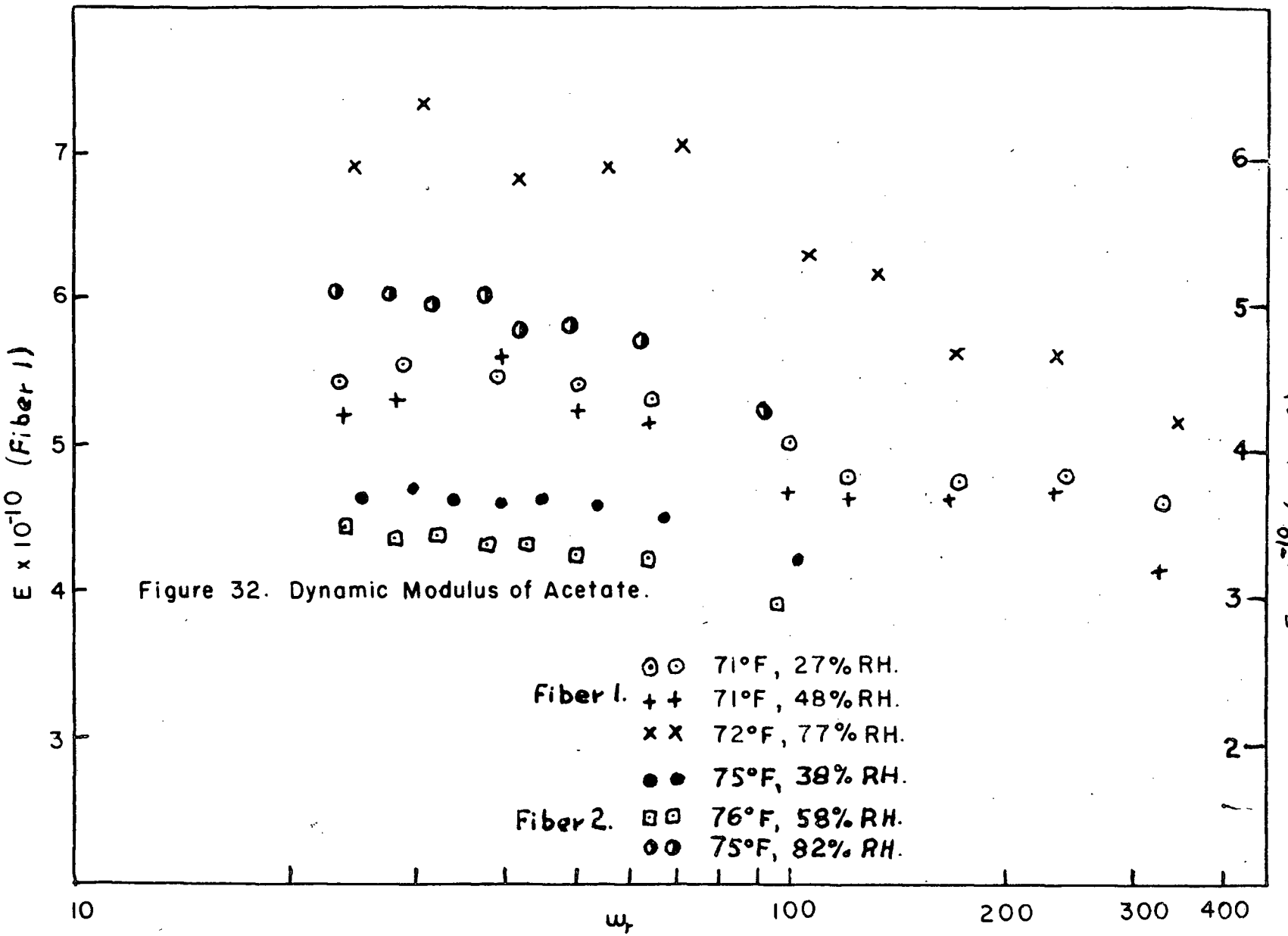

Figure 32. Dynamic Modulus of Acetate.

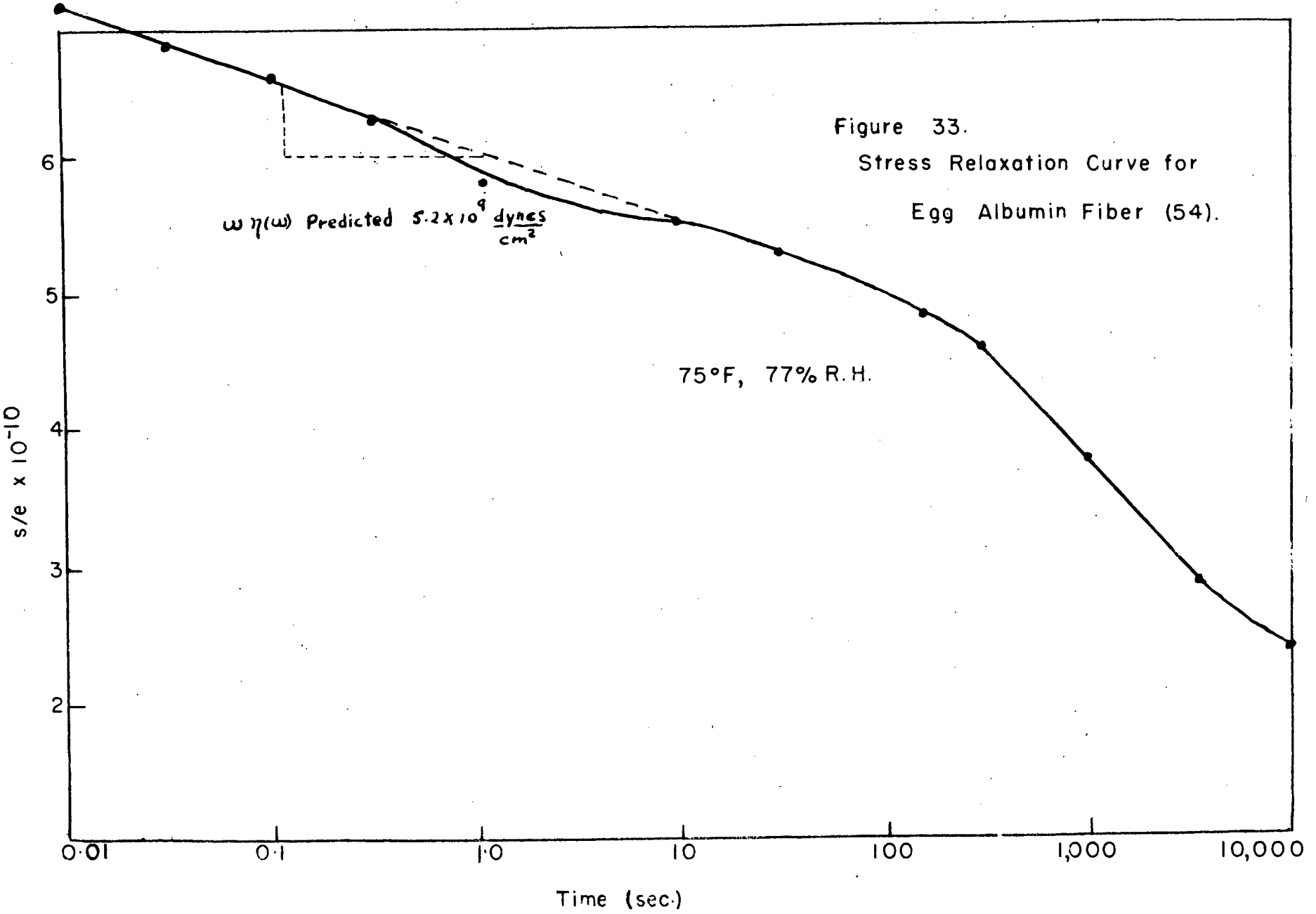

Figure 33.
Stress Relaxation Curve for
Egg Albumin Fiber (54).

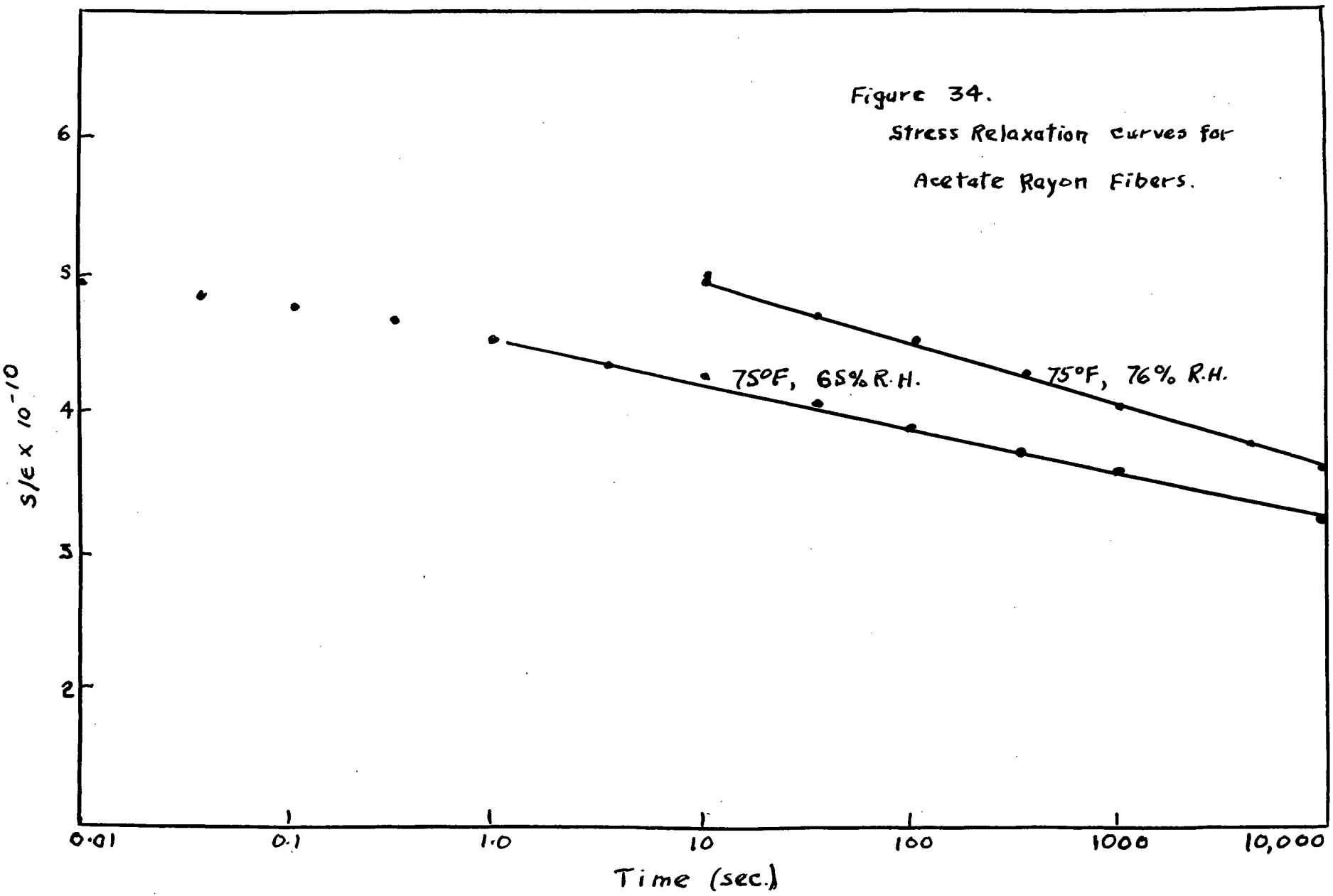

Figure 34.
Stress Relaxation curves for
Acetate Rayon Fibers.

DISCUSSION OF RESULTS

The fact that the plots of log $\eta(\omega)$ against log ω_r are linear with a slope of about -1 verifies the approximate hyperbolic relation between the internal viscosity and frequency as described by Kuhn et al (Appendix). Deviations of the slopes from the value of -1 is not understood, but may be caused by approximations made in determining the distribution of relaxation times.

Verification has also been found for the predicted independency of dynamic modulus on frequency. The slight decrease in modulus at higher frequencies is caused by the difficulty in determining accurately the effective mass of the vibrator unit.

From the equation:

$$E(\omega) = \frac{\ell(\omega_r^2 + g/h)}{2A}(M + m)$$

where M mass added to unit to lower the resonance frequency

m mass of vibrator unit

g/h gravitational constant/height of suspension

A cross-sectional area of fiber

ℓ length of fiber

ω_r resonance frequency

it is easily seen that, when M is large (20 to 100 gm. at low frequencies), any discrepancy from the true value of m will have an insignificant effect on $E(\omega)$ but, when M is small (0 to 10 gm. at higher frequencies), the effect on $E(\omega)$ will increase as M is decreased to zero. The accuracy of determining m is 7% and, in general, the values of $E(\omega)$ obtained vary about 10% from high to low resonance frequencies.

In addition, at constant strain amplitude, the actual vibrational amplitude decreases at higher frequencies because the length of fiber being vibrated is being decreased. This increases the % error in determining the resonance frequency.

The energy loss factor, $\omega\eta(\omega)$, increases with relative humidity but, as shown in Figure 29, the variation is within the fiber to fiber variation which in turn is probably caused by irregularity of cross-sectional area. This explains the apparent absence of the same regularity of the humidity effect in Figure 27, the data for which were obtained using different fibers for each experiment. This increase is expected because $\eta(\omega)$ depends on the magnitude of the quantity $\frac{d\epsilon}{d\tau}$, appearing in Equation 22 of the appendix, or the slope of the creep curve. As shown in Table IV, it has been found that fibers creep faster at higher humidities, and hence $\omega\eta(\omega)$ should increase with humidity.

TABLE IV

Elongation of Acetate under 10 gm. Tensioning Weight for 18 Hours

38% RH.	1.543 mm.
58% RH.	3.512 mm.
82% RH.	9.850 mm.

An increase in the energy loss factor has also been found by Honold and Wakeham [27] from comparison of stress-strain hysteresis curves of wet and dry fibers.

The predicted value of $\omega\eta(\omega)$ for "albumin (54)" at 77% RH. 5.0×10^9 dynes/cm^2 (Figure 33) does not compare too favorably with the experimentally determined value of 1.2×10^9 dynes/cm^2 (Figure 28) . For acetate the values of $\omega\eta(\omega)$ predicted, 3.0×10^9 dynes/cm^2 at 65% RH. and 4.5×10^9 at 76% RH. (Figure 34), compare more favorably with those experimentally determined, 2.24×10^9 dynes/cm^2 at 67% RH. (Figure 27) and 2.15×10^9 at 77% RH. (Figure 29). Because of the fiber to fiber variation of the energy loss factor, exact agreement cannot be expected unless both relaxation and vibrational curves are obtained from experiments on the same fiber.

The theory assumes the presence of frictional forces of a viscous nature (dissipative factor proportional to velocity of deformation) and neglects any solid friction effects (dissipative factor independent of rate of deformation). Dunell and Dillon investigated the possibility of the presence of solid friction effects in the vibrational experiments and found them to be absent in most fibers studied or only a small fraction of the energy lost per cycle. In addition, the theory assumes Newtonian viscosity which is the limiting case of the hyperbolic sine law used by Eyring et al [28] to discuss the stress relaxation and stress-strain curves of acetate. It seems reasonable, however, to assume Newtonian behaviour for the small strain amplitudes used in this investigation.

The effect of orientation on $\omega\eta(\omega)$ for the albumin fibers is as expected. The more highly oriented fiber has fewer relaxation mechanisms and approaches more closely the behaviour of an ideal spring. The relaxation curve would have a smaller slope and this would cause the $\omega\eta(\omega)$ factor to have a smaller value.

It has been found that the dependence of dynamic modulus on relative humidity is not explainable in terms of the present theory of the mechanical behaviour of polymer systems. The equation:

$$E_{dyn} = E_1 + E^\circ \log \frac{1 + \omega^2 \tau_m^2}{1 + \omega^2 \tau_l^2}$$

for the dynamic modulus discussed in the Introduction reduces to:

$$E_{dyn} = E_1 + E^\circ \log \tau_m + E^\circ \log \omega$$

with the restrictions:

$$\omega\tau_m \gg 1 \qquad \text{and} \qquad \omega\tau_l \ll 1$$

E° is the slope of the stress relaxation curve, τ_m and τ_l are the maximum and minimum times of the relaxation spectrum, E_1 takes into account any residual stress (in the event that the stress does not decay to zero as shown in Figure 4 but approaches asymptotically some value greater than zero) and ω is the frequency at which the modulus is measured.

With the assumption that the variation with relative humidity of $\omega\eta(\omega)$, which according to theory is equal in magnitude to the slope of the stress relaxation curve, is correct, it is found that E_{dyn} calculated from the slopes and the corresponding maximum relaxation times should be essentially the same at all humidities. This, of course, is in agreement with the initial assumption of Hookean behaviour of any elastic mechanisms.

For this calculation, the values of $\omega\eta(\omega)$ for acetate, which are directly proportional to the decrease in stress per cycle of log time at each relative humidity, were obtained from Figure 29. On the basis of these rates of stress decay, relaxation times, τ_m^*, the time required for the stress to decay to zero, were next calculated. Because of the geometry of the stress relaxation diagram,

$$E^\circ \log \tau_m^* = E_1 + E^\circ \log \tau_m$$

where E_1, as before, is any residual stress greater than zero and τ_m is the relaxation time obtained by extrapolation of the stress relaxation curve to E_1 instead of to zero stress. Thus, $E^\circ \log \tau_m^*$ will completely define the contributions to E_{dyn} of the relaxation mechanisms and any residual stress. The results of this calculation are summarized in Table V.

TABLE V

	$E^\circ \propto \omega\eta(\omega)$	$E^\circ \log \omega$	$E_1 + E^\circ \log \tau_m$	E_{dyn}
39% RH.	0.125×10^{10}	0.09×10^{10}	4.75×10^{10}	4.87×10^{10}
48% RH.	0.17	0.10	4.76	4.86
77% RH.	0.23	0.16	4.60	4.76

The variation of E_{dyn} with relative humidity of acetate at the lower humidities is small (5%) and, considering the many approximations made, conforms to the theory but the large increase at the higher humidities for acetate and the significant decrease in the modulus of the albumin fibers at the higher humidities are inexplicable on the basis of the present theory.

The dependence of E_{dyn} on temperature, in agreement with the work of other investigators (17, 29, 30), has been found to be negligible for small temperature variations.

The increase in dynamic modulus of egg albumin fibers expected from increased orientation and accompanying increase in degree of crystallinity has not been found.

APPENDIX

DETERMINATION OF DYNAMIC PARAMETERS FROM CREEP EXPERIMENTS BY THE METHOD OF KUHN, KÜNZLE AND PREISMANN.

For this analysis the simple expression:

$$E = \frac{s}{\epsilon} \qquad (1)$$

is replaced by:

$$\frac{s}{\epsilon} = \sum E_{io} e^{-\frac{t}{\tau_i}} \qquad (2)$$

where the elastic modulus is now time dependent. E_{io} is called the partial elastic modulus belonging to the ith component in the infinite array and τ_i is the constant relaxation time of that unit. In the limit, the summation in (2) can be replaced by an integral:

$$E(t) = \int_0^\infty \frac{dE_o}{d\tau} e^{-\frac{t}{\tau}} d\tau \qquad (3)$$

where $\frac{dE_o}{d\tau}$ is the sum of those components of the elastic modulus arising in the interval between τ and $\tau + d\tau$ of the entire spectrum; ie. it is the distribution density of the partial elastic moduli. Since the values of τ_i in (2) assume all possible discrete values, the integral in (3) must have the limits zero and infinity. For the ideal case when t, the time between initia- of the elongation and measurement of the tension is zero, then:

$$E = E_0 = \sum E_{i0} \qquad (4)$$

It is seen from (2) and (3) that we can predict the elastic behaviour of a substance as soon as the relaxation time spectrum, ie. all values of E_{i0} and τ_i in (2) or the magnitude of $\frac{dE_0}{d\tau}$ in (3), is given as a function of time.

An increment of stress in a time element dt is given by:

$$\frac{ds}{dt} \cdot dt = \frac{d\epsilon}{dt} \cdot dt \sum E_{i0} \qquad (5)$$

and this increment decays in a time period $t = t_1$ to $t = t_1$, if the strain is constant at t_1, by an amount:

$$ds = \frac{d\epsilon}{dt} \cdot dt \sum E_{i0} e^{-(t_1 - t)/\tau_i} \qquad (6)$$

The final stress at the time t_1 is found by evaluating the integral:

$$S_{t_1} = \int_0^{t_1} \frac{d\epsilon}{dt} \sum E_{i0} e^{-(t_1 - t)/\tau_i} dt \qquad (7)$$

On the basis of a continuous distribution of relaxation times, substitution of (3) in (7) yields:

$$S_{t_1} = \int_0^{t_1} \frac{d\epsilon}{dt} \int \frac{dE_0}{dt} e^{-(t_1 - t)/\tau_i} d\tau \, dt \qquad (8)$$

Similarly, if a shearing force at any instant t_1 is F_{t_1} and $\frac{d\gamma}{dt}$ is the rate of shear, then:

$$F_{t_1} = \frac{1}{2(1+\mu)} \int_0^{t_1} \frac{d\gamma}{dt} \sum E_{i0} e^{-(t_1 - t)/\tau_i} dt \qquad (9)$$

where μ is Poisson's ratio.

Assuming t_1 is large compared to the τ_i's derived from the spectrum then, for $\frac{d\gamma}{dt}$ constant in the interval zero to t_1, (9) becomes:

$$F_{t_1} = \frac{1}{2(1+\mu)} \frac{d\gamma}{dt} \sum E_{i0} \tau_i \qquad (10)$$

Thus the force exerted per cm^2 becomes simply a constant flow velocity independent of any chosen t_1 provided the restriction $t_1 \gg \tau_i$ is observed.

Such a relation holds for Newtonian fluids whose viscosity is defined as:

$$\eta = \frac{F}{d\gamma/dt} \qquad (11)$$

Comparison of (10) and (11) gives:

$$\eta = \frac{1}{2(1+\mu)} \sum E_{i0} \tau_i \qquad (12)$$

Therefore it is seen that the viscous nature of a material can be determined from the relaxation time distribution. For a continuous distribution of τ_i's (12) becomes:

$$\eta = \frac{1}{2(1+\mu)} \int_0^{\tau_i'} \frac{dE_0}{d\tau} \tau \, d\tau \qquad (13)$$

where it is assumed that the distribution has an upper limit, τ_i', and that the time between flow initiation and measurement of the shear force is large compared to τ_i'.

If the condition $t_1 \gg \tau_i$ is not fulfilled but $\frac{d\gamma}{dt}$ is still held constant, (9) is still valid but the shearing force is now dependent on both t_1 and viscosity. The contribution to F_{t_1} of a connecting mechanism for which $\tau_k \gg t_1$ is:

$$(F_{t_1})_K = \frac{1}{2(1+\mu)} \frac{d\gamma}{dt} t_1 E_{K0} \qquad (14)$$

which, on comparison to (5), is merely a contribution to an elastic mechanism.

If, for (8) and (9), the rate of elongation, $\frac{d\epsilon}{dt}$, and shear velocity, $\frac{d\gamma}{dt}$, are not constant in the time interval zero to t_1 but are replaced by periodic functions of time, "dynamic" parameters are obtained which are time dependent. If, for example, $\gamma = \gamma_0 \sin \omega t$ (15) from which:

$$\frac{d\gamma}{dt} = \gamma_0 \omega \cos \omega t \qquad (16)$$

The contribution of the kth unit to the shear force will be given by (cf 9):

$$(F_{t_1})_K = \frac{\gamma_0 \omega E_{K0}}{2(1+\mu)} \cdot \frac{1}{\tau_K} \cdot \frac{\cos \omega t + \omega \sin \omega t}{\left(\frac{1}{\tau_K}\right)^2 + \omega^2} - \frac{\gamma_0 \omega E_{K0} e^{-t_1/\tau_K}}{\tau_K \left[2(1+\mu)\frac{1}{\tau_K^2} + \omega^2\right]}$$

If the time between the initiation of the oscillatory shear and the measurement of the tension is large compared to the period of shear, $T = \frac{2\pi}{\omega}$, ie. the measurements are made only after several cycles, the second fraction of (16) becomes negligible and F_{t_1} then depends only on the first fraction.

The mechanical energy lost per cm^3 of the material due to the kth unit during a period t_1 to $t_1 + \frac{2\pi}{\omega}$ will be given by:

$$\left(\frac{dA}{dt} \frac{2\pi}{\omega}\right)_K = \omega \gamma_0^2 \frac{E_{K0}}{2(1+\mu)} \cdot \frac{\frac{\pi}{\tau_K}}{\frac{1}{\tau_K^2} + \omega^2} \qquad (17)$$

The accompanying work per cm^3 per second is obtained by multiplication of (17) by $\frac{\omega}{2\pi}$:

$$\left(\frac{dA}{dt}\right)_k = \frac{\omega^2 \gamma_0^2 E_{k0}}{4(1+\mu)} \cdot \frac{\tau_k}{\omega^2 \tau_k^2 + 1} \qquad (18)$$

By summing over all k, the work transformed into heat per cm^3 per second due to shear is:

$$\frac{dA}{dt} = \frac{\omega^2 \gamma_0^2}{2} \cdot \frac{1}{2(1+\mu)} \sum \frac{E_{i0} \tau_i}{\omega^2 \tau_i^2 + 1} \qquad (19)$$

For a material having viscosity η, the work dissipated as heat is found (from 11 and 15) to be:

$$\frac{dA}{dt} = F \frac{d\gamma}{dt} = \eta \left(\frac{d\gamma}{dt}\right)^2 = \frac{1}{2} \omega^2 \gamma_0^2 \eta \qquad (20)$$

Comparison of (19) and (20) yields:

$$\eta = \frac{1}{2(1+\mu)} \cdot \sum \frac{E_{i0} \tau_i}{\omega^2 \tau_i^2 + 1} \qquad (21)$$

or, assuming again a continuous spectrum of relaxation times:

$$\eta = \frac{1}{2(1+\mu)} \int_0^\infty \frac{dE_0}{d\tau} \frac{\tau}{\omega^2 \tau^2 + 1} d\tau \qquad (22)$$

The relations (21) and (22) are generalizations of (12) and (13) since, if $\tau \ll \frac{1}{\omega}$, then $\omega\tau \ll 1$ and the former pair reduces to the latter. These equations show that the viscosity measured by the damping in periodic shear is in general dependent on the frequency and that this frequency dependence is totally determined by the relaxation time spectrum.

If the sample is stretched periodically rather than

subjected to shear, analogous to the above derivation, the mechanical energy transformed into heat by a periodic extension will be:

$$\frac{dA}{dt} = \frac{1}{2}\omega^2\epsilon_o^2 \sum \frac{E_{io}\tau_i}{\omega^2\tau_i^2+1} \qquad (24)$$

and for a continuous distribution of relaxation times:

$$\frac{dA}{dt} = \frac{1}{2}\omega^2\epsilon_o^2 \int_0^\infty \frac{dE_o}{dt}\frac{\tau}{\omega^2\tau^2+1}\,d\tau \qquad (25)$$

Brenschede[32] found that between 10^{-2} and 10^4 sec. the creep curve for rubber was adequately represented by the empirical relation:

$$\frac{1}{E'} = \frac{a + b\ln t}{b} \qquad (26)$$

where E' is the creep modulus and a and b are empirical constants. Since this equation is undefined for $t = 0$, it is arbitrarily transformed to:

$$\frac{1}{E'} = a + \ln t - E_i(-ct) \qquad (27)$$

or:

$$\epsilon = \frac{S}{E'} = \frac{S}{b}\left[a + \ln t - E_i(-ct)\right. \qquad (27a)$$

for which $\ln c = a - \ln\xi$ and ξ is Euler's constant and E_i is the exponential integral:

$$-E_i(-x) = \int_x^\infty \frac{e^{-u}}{u}\,du \qquad (28)$$

Expression (27a) remains finite for $t=0$ and for small values of time becomes identical with (27).

Now, on the basis of (27a):

$$\frac{d\epsilon}{dt} = \frac{s}{b}\left(\frac{1-e^{-ct}}{t}\right) \tag{29}$$

which indicates that the rate of strain remains finite for $t = 0$, and for large values of time can be replaced by:

$$\frac{d\epsilon}{dt} = \frac{s}{b}\frac{1}{t} \tag{30}$$

Referring back to (8) and using (29), the shear stress after time t_1 will be given by:

$$s_{t_1} = \int_0^{t_1} \frac{s}{b}\frac{1-e^{-ct}}{t} \int_0^{\infty} \frac{dE_0}{dt} e^{-(t_1-t)/\tau}\, d\tau\, dt \tag{31}$$

By means of the Laplace Transformation, Kuhn et al obtained a continuous function satisfying this last equation:

$$E(t) = \int_{\frac{1}{c}}^{\infty} \frac{b\, e^{-t/\tau}}{\tau[\ln^2(c\tau-1)+\pi^2]}\, d\tau \tag{32}$$

Comparison of this equation with (3) shows that for $\tau > \frac{1}{c}$:

$$\frac{dE_0}{dt} = \frac{b}{\tau}\frac{1}{\ln^2(c\tau-1)+\pi^2} \tag{33}$$

and for $0 < \tau < \frac{1}{c}$:

$$\frac{dE_0}{dt} = 0 \tag{33a}$$

These two equations agree with that empirically determined from the flow diagram. According to (33a) the continuum is bounded by $\tau = \frac{1}{c}$ for which the distribution density, $\frac{dE_0}{dt}$, vanishes. This limit is caused by the arbitrary replacement of (26) by (27)

and has no theoretical significance. The constants a and b can be determined experimentally from creep curves at constant stress using the empirical relation of Brenschede.

Substitution of (33) and (33a) into (22) gives:

$$\eta = \frac{1}{2(1+\mu)} \int_{\frac{1}{c}}^{\infty} \frac{b}{\tau} \frac{1}{\ln^2(c\tau - 1) + \pi^2} \cdot \frac{\tau\, d\tau}{\omega^2\tau^2 + 1} \qquad (34)$$

Letting $T_s = \frac{2\pi}{\omega}$, the viscosity, in terms of the period of vibration becomes:

$$\eta = \frac{1}{2(1+\mu)} \frac{b}{a^2} \cdot \frac{T_s}{4} \qquad (35)$$

Substitution of (34) into (20) gives for shear:

$$\frac{dA}{dt} = \frac{\omega\pi}{2(1+\mu)} \cdot \frac{b}{a^2} \cdot \frac{\gamma_0^2}{4} \qquad (36)$$

and:

$$\frac{dA}{dt} = \frac{\omega\pi}{8} \cdot \frac{b}{a^2} \epsilon_0^2 \qquad (37)$$

as the energy lost per sec. in compression or extension. Thus, the viscosity is a hyperbolic function of the frequency and the energy is directly proportional to the frequency and to the square of the amplitude of deformation.

Making the following assumptions, Kuhn et al show that $E(t)$ in equation (32) is identical to the creep modulus of Brenschede.

$$e^{-t/\tau} = 0 \quad (t/\tau > 1)$$
$$= 1 \quad (t/\tau < 1)$$
$$\ln c \doteq a$$

Therefore, the modulus from relaxation at constant strain is the

same as that from creep at constant stress.

The elastic modulus in equation (32) is a function of time but, as was shown previously, we can obtain a modulus which is independent of the length of the experiment by using periodic stresses., Then $E(t)$ depends in general on the frequency. In this case:

$$E(\omega) = \frac{b}{\ln c - \ln \omega} \qquad (\ln c - \ln \omega >> 1)$$

If the period of vibration is such that $\ln c >> \ln \omega$, then:

$$E(\omega) \doteq \frac{b}{a}$$

Hence, the dynamic modulus, in the region of applicability of (33a) is independent of the frequency.

BIBLIOGRAPHY

(1) Mark, Am. J. Phys., 13, 207 (1945).

(2) Mark, Ind. Eng. Chem., 34, 449 (1942).

(3) Simha, Ann. N.Y. Acad. Sci., 44, 263, 297 (1943).

(4) Flory and Rehman, Ann. N.Y. Acad. Sci., 44, 419 (1943).

(5) Gehman, Jones and Woodford, Ind. Eng. Chem, 35, 946 (1943).

(6) Mooney, J. App. Phys., 19, 434 (1948).

(7) Powell, Clark and Eyring, J. Chem. Phys., 9, 268 (1941).

(8) Flory, J. Chem. Phys., 10, 51 (1942).

(9) Mochulsky and Tobolsky, Ind. Eng. Chem., 40, 2155 (1948).

(10) Flory, J. Chem. Phys., 10, 660 (1942).

(11) Roscoe, Brit. J. App. Phys., 1, 171 (1950).

(12) Macey and Reiner, Brit., J. App. Phys., 1, 332 (1950)

(13) Mark, Chem. Rev., 25, 121 (1939).

(14) Andrews, Hoffmann-Bang and Tobolsky, J. Polymer Sci., 3, 669 (1948).

(15) Brown and Tobolsky, J. Polymer Sci., 6, 165 (1951).

(16) Tobolsky and Eyring, J. Chem. Phys., 11, 125 (1945).

(17) Kuhn, Künzle and Preismann, Helv. Chim. Acta, 30, 307, 464, 839 (1937).

(18) Dunell and Andrews, Textile Research J., 21, 404 (1951).

(19) Lundgren, Textile Reseach J., 15, 335 (1945).

(20) Bergmann and Niemann, J. Biol. Chem., 118, 301 (1937).

(21) Brand and Kassel, J. Biol. Chem., 133, 437 (1940).

(22) Kibrick, J. Biol. Sci., 152, 411 (1944).

(23) Palmer and Galvin, J. Am. Chem. Soc., 65, 2187 (1943).

(24) Lyons and Prettyman, J. App. Phys., 18, 586 (1947).

(25) Dunell and Dillon, Textile Research J., 21, 393 (1951).

(26) Dillon, Prettyman and Hall, J. App. Phys., 15, 309 (1944).

(27) Honold and Wakeham, Ind. Eng. Chem., 40, 131 (1948).

(28) Eyring, White, Halsey, Stein and Reichardt, Textile Research Journal, 15, 295, 451 (1946); 16, 13, 53, 124, 201, 329, 335, 378, 382, 635 (1948).

(29) Yousef, Phil. Mag., 37, 490 (1946).

(30) Mooney, J. App. Phys., 19, 434 (1948).

(31) Private Communication with Dr. H.P. Lungren.

(32) Brenschede, Kolloid Zeit., 104, 1 (1943).